The Meteoritical Society

Meteoritics & Planetary Science 56, Nr 6, 1005–1023 (2021)
doi: 10.1111/maps.13661

Extraterrestrial hydroxy amino acids in CM and CR carbonaceous chondrites

Toshiki KOGA[1]*, Eric T. PARKER[2], Hannah L. McLAIN[2,3], José C. APONTE[2,3], Jamie E. ELSILA[2], Jason P. DWORKIN[2], Daniel P. GLAVIN[2], and Hiroshi NARAOKA[1]

[1]Department of Earth and Planetary Sciences, Kyushu University, 744 Motooka, Nishi-ku, Fukuoka 819-0395, Japan
[2]NASA Goddard Space Flight Center, Greenbelt, Maryland 20771, USA
[3]Catholic University of America, Washington, District of Columbia 20064, USA
*Corresponding author. Email: koga.toshiki.590@s.kyushu-u.ac.jp; kogatoshiki590@gmail.com

(Received 03 February 2021; revision accepted 14 April 2021)

Abstract–The abundances, distributions, and enantiomeric ratios of a family of three- and four-carbon hydroxy amino acids (HAAs) were investigated in extracts of five CM and four CR carbonaceous chondrites by gas chromatography-mass spectrometry analyses. HAAs were detected in both the acid hydrolysates of the hot water extracts and the 6 M HCl extracts of all the CM and CR chondrites analyzed here with total hot water and HCl extractable HAA concentrations ranging from 6.94 to 315 nmol g^{-1}. The HAA analyses performed in this study revealed: (1) the combined (hot water + HCl) extracts of CR2 chondrites contained greater abundances of α-HAAs than that of CM2 chondrites and (2) the combined extracts of CM and CR chondrites contained roughly similar abundances of β- and γ-HAAs. Application of the new GC-MS method developed here resulted in the first successful chromatographic resolution of the enantiomers of an α-dialkyl HAA, D,L-α-methylserine, in carbonaceous chondrite extracts. Meteoritic α-methylserine was found to be mostly racemic within error and did not show L-enantiomeric excesses correlating with the degree of aqueous alteration, a phenomenon observed in meteoritic isovaline, another α-dialkyl amino acid. The HAAs identified in CM and CR chondrite extracts could have been produced during parent body alteration from the Strecker cyanohydrin reaction (for α-HAAs) and an ammonia-involved formose-like reaction (for β-, and γ-HAAs).

INTRODUCTION

Amino acids are among the most intriguing soluble organic compounds found in meteorites and provide clues regarding the chemical evolution processes in the early solar system that likely set the stage for the origin of life (Chyba and Sagan 1992). The amino acid compositions of a variety of carbonaceous chondrites have been extensively examined over the past 50 yr. During this period, analytical methods for amino acids have continuously improved, enabling the ability to chromatographically separate amino acid structural isomers and enantiomers, and to detect trace quantities of amino acids (e.g., Glavin et al. [2018] and references therein; Simkus et al. [2019]; Glavin et al. [2020a, 2020b]).

By applying increasingly improved analytical techniques to study the amino acid chemistry of meteorites, new information has been revealed to suggest that the distribution of structural isomers of meteoritic amino acids provides insight into the formation mechanisms of these aliphatic compounds and the possible processing histories of the meteorite parent bodies (Elsila et al. [2016] and references therein). For example, the relative abundances of the C_5 amino acid isomers as a function of amine position (α-, β-, γ-, δ-) are significantly different between unaltered and aqueously altered carbonaceous chondrites (Glavin et al. 2006, 2010; Glavin and Dworkin 2009; Burton et al. 2014). The less or moderately aqueously altered carbonaceous chondrites (e.g., CM2, CR2, and CR3) possess an amino acid distribution that is dominated by α-amino acids (Glavin et al. 2006, 2010). For example, the CM2 Murchison meteorite possesses predominantly α-amino acids, including glycine, alanine, and α-aminoisobutyric acid, which were hypothesized to have

formed by the Strecker cyanohydrin synthesis, based on the coexistence of their corresponding α-hydroxy acids and α-iminodicarboxylic acids that are also products of Strecker synthesis (Peltzer and Bada 1978; Peltzer et al. 1984; Lerner and Cooper 2005). In contrast, the heavily aqueously altered chondrites (e.g., CI1, CM1, and CR1) possess greater relative abundances of β-, γ-, and δ-amino acids compared to α-amino acids (Glavin et al. 2006, 2010; Elsila et al. 2016). This observation may be due to the hydrolysis of lactams and the thermal decarboxylation of α-amino dicarboxylic acids (Cooper and Cronin 1995; Glavin et al. 2010), or may correspond to differences in their degradation rates under hydrothermal conditions (Li and Brill 2003). In either scenario, amino acid syntheses and degradations require exposure of the precursor compounds, and amino acids themselves, to liquid water (Glavin et al. 2018). Therefore, the aqueous alteration of meteorite parent bodies is thought to play a crucial role in influencing the distributions of meteoritic amino acids (Botta and Bada 2002; Elsila et al. 2016).

It has also been hypothesized that the extent to which meteorite parent bodies have undergone aqueous alteration may correspond to observed L-enantiomeric excesses of extraterrestrial amino acids (Glavin and Dworkin 2009). Many amino acids possess a property known as chirality, whereby the chemical compound is composed of two non-superimposable mirror-image structures, or enantiomers. These enantiomers are distinguished as the so-called L-amino acids ("left-handed") or D-amino acids ("right-handed"). Terrestrial life uses L-enantiomers almost exclusively as a component of proteins, whereas abiotically synthesized amino acids contain an equal (racemic) mixture of both enantiomers, unless biology or special conditions are used to induce asymmetry. Therefore, chirality is a critical chemical property to monitor when assessing the origins of potential biomolecules.

An example of a meteoritic amino acid that is a useful target analyte to evaluate for potential enantiomeric excesses is the non-proteinogenic amino acid isovaline, which is rare in the terrestrial biosphere (Pizzarello et al. 2003; Elsila et al. 2012). Different laboratories have reported that isovaline has various L-enantiomeric excesses ranging from 0% to ~20%, with an increase in L-enantiomeric excess roughly correlating with an increased degree of aqueous alteration among the carbonaceous chondrites analyzed (Elsila et al. [2016] and references therein). More specifically, unaltered CM and CR type 3 (petrologic type ≥2.6, see discussion below) carbonaceous chondrites show racemic isovaline, but more aqueously altered type 1 or type 2 carbonaceous chondrites (petrologic type 2.0–2.5, see discussion below) contain L-isovaline excesses (Glavin and Dworkin 2009; Glavin et al. 2010, 2020b; Martins et al. 2015).

Although aliphatic amino acids have been thoroughly investigated in carbonaceous chondrites, hydroxyl (–OH) group-bearing amino acids known as HAAs have been understudied except for serine and threonine, which are common proteinogenic amino acids. Koga and Naraoka (2017) revealed the distribution of HAAs in extracts of the Murchison meteorite, including nine newly identified C_3 and C_4 HAAs with α-, β-, and γ-amino group positions (Fig. 1). It is worth noting that HAAs were detected not only in the acid hydrolysates of the hot water extracts, but were also present at comparable or greater abundances in the 6 M HCl extracts of the meteorite residues that had previously experienced hot water extraction (Koga and Naraoka 2017).

There have been limited efforts to detect and quantify amino acids in aqueous HCl extracts of meteorites (Engel and Nagy 1982; Bada et al. 1998; Glavin et al. 1999; Koga and Naraoka 2017). However, those few explorations have yielded intriguing results. For example, Glavin et al. (1999) reported that HCl extraction of chondrites resulted in decreased amino acid abundances compared to the same samples being treated by hot water extraction followed by acid hydrolysis. It was proposed that this decreased amino acid abundance may be partially explained by potential amino acid degradation processes that might have occurred during HCl extraction (Glavin et al. 1999). Details pertaining to such representative HCl extraction procedures are provided elsewhere (Bada et al. 1998; Glavin et al. 1999). Additionally, what has been learned from investigating the aqueous HCl extract of the Murchison meteorite is that HAAs represent a new subclass of meteoritic amino acids that are not necessarily fully released from the meteorite matrix by hot water extraction alone (Koga and Naraoka 2017). However, it remains unknown what abundances and distributions of structural isomers of HAAs exist in carbonaceous chondrites other than the CM2 Murchison meteorite. Moreover, enantiomeric analyses of HAAs by gas chromatography-mass spectrometry (GC-MS) have been sparsely executed in previous studies, except for targeted searches for serine and threonine (Pizzarello et al. 2012). In this study, we developed a new GC-MS method to investigate the abundances of three- and four-carbon (C_3-C_4) HAA structural isomers and the enantiomeric compositions of chiral HAAs in CM and CR chondrites ranging from type 1 to type 2. This approach allows for the evaluation of the molecular distributions and possible formation pathways of HAAs across a range of carbonaceous chondrites that experienced different degrees of parent body alteration.

α-amino	β-amino	γ-amino
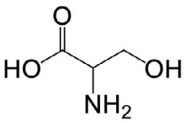 Serine	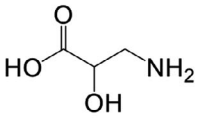 Isoserine*	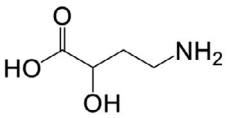 4-Amino-2-hydroxy-butanoic acid*
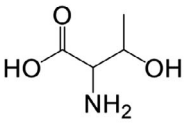 Threonine	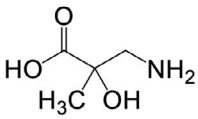 α-Methylisoserine**	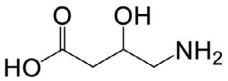 4-Amino-3-hydroxy-butanoic acid*
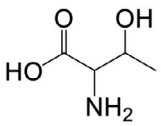 *allo*-Threonine	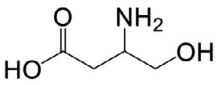 β-Homoserine*	
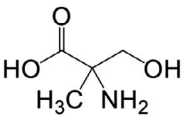 α-Methylserine*	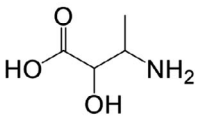 Isothreonine*	
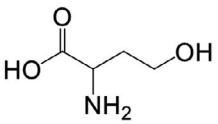 Homoserine*	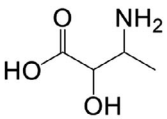 *allo*-Isothreonine*	
	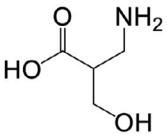 3-Amino-2-(hydroxy-methyl)propanoic acid*	

Fig. 1. All the structural isomers of C_3 and C_4 hydroxy amino acids investigated in this study. *Hydroxy amino acids identified in the Murchison (CM2) meteorite by Koga and Naraoka (2017). **Although a peak whose mass spectrum corresponding to the structure of α-methylisoserine was detected in the Murchison meteorite by Koga and Naraoka (2017), proper identification of the peak was not possible in that reporting due to the unavailability of the necessary analytical standard.

MATERIALS AND METHODS

Chemicals and Reagents

Commercial standards of HAAs were purchased from various manufacturers as follows: Sigma-Aldrich: D,L-α-methylserine (>99% purity), D-threonine (>98% purity), L-threonine (>98% purity), D,L-*allo*-threonine (>99% purity), D,L-isoserine (>98% purity), D,L-homoserine (>99% purity), D-β-homoserine (>99% purity), L-β-homoserine (>99% purity); Tokyo Chemical Industry (TCI): D,L-4-amino-3-hydroxybutanoic acid (4-A-3-HBA) (>98% purity); Enamine Ltd.: a combined D, L-isothreonine and D,L-*allo*-isothreonine standard (>95% purity); and Fluka: D,L-serine (>99% purity). Racemic standards for 3-amino-2-(hydroxymethyl)propanoic acid (3-A-2-HMPA) and 4-amino-2-hydroxybutanoic acid (4-A-2-HBA) were not commercially available, so the following enantiopure standards of these amino acids were purchased from Sigma-Aldrich: D-3-A-2-HMPA (>96% purity) and L-4-A-2-HBA (>96% purity). The standard for D,L-α-methylisoserine was obtained by hydrolysis of D,L-methyl-3-amino-2-hydroxy-2-methylpropanoate hydrochloride (>97% purity, Aurum Pharmatech LLC) via 6 M HCl vapor hydrolysis at 150 °C for 3 h (Glavin et al. 2006). A stock mixed HAA solution (~8 μM per analyte) was prepared by combining individual HAA standards described above in Millipore Integral 10 ultrapure water (18.2 MΩ, <3 ppb total organic carbon). As an internal standard, a stock solution of 8-aminooctanoic acid (8-AOA; >99%, Sigma-Aldrich) was prepared with the same concentration (~8 μM).

All glassware and sample handling tools were rinsed with Millipore Integral 10 ultrapure water (18.2 MΩ-cm, ≤3 ppb total organic carbon), wrapped in aluminum foil, and heated at 500 °C, in air, overnight, to remove organic contamination. Preparation of reagents used to perform acid vapor hydrolysis (Glavin et al. 2006) and desalting by cation exchange chromatography (Glavin et al. 2006; Simkus et al. 2019) are described elsewhere. Acid extraction was performed using 6 M double-distilled HCl (ddHCl). Precolumn derivatization of samples before GC-MS analyses involved the use of acetyl chloride (Acros Organics, ≥99%), isopropanol (Sigma-Aldrich, ≥99%), heptafluorobutyric anhydride (HFBA, Sigma-Aldrich, ≥98%), and chloroform (Sigma-Aldrich, for HPLC, ≥99.9%).

Meteorite Samples and Sample Preparation

The interior chips of five CM and four CR chondrites, none of which contained visible evidence of fusion crust, were used for HAA analyses in this study (Table 1). The Antarctic CM2 chondrites, Asuka 881458 (A-881458) and Yamato 791198 (Y-791198), were provided by the Antarctic meteorite curator at the National Institute of Polar Research (NIPR) in Tokyo, Japan. All other meteorites, including the other Antarctic CM2 chondrites: Lewis Cliffs (LEW) 90500 and Lonewolf Nunataks (LON) 94101, the CM 1/2 chondrite: Allan Hills (ALH) 83100, the CR2 chondrites: Miller Range (MIL) 07525, Meteorite Hills (MET) 00426, and LaPaz Icefield (LAP) 02342, and the CR1 chondrite: Grosvenor Mountains (GRO) 95577 were provided by the Antarctic meteorite curator at the NASA Johnson Space Center. The petrologic subtype assignments of these carbonaceous chondrites were suggested by several previous studies, as summarized in Table 1. In this study, the CR chondrite subtype classifications were based on the alteration metrics proposed by Harju et al. (2014), Howard et al. (2015), and Alexander et al. (2013). The CM chondrite subtype classifications that were available in the literature and used in Table 1 were based on the aqueous alteration metrics described by Rubin et al. (2007), Howard et al. (2015), and Alexander et al. (2013). Although the subtype for A-881458 was not available, this meteorite has been classified as a weakly heated CM2 chondrite (Nakamura 2005; Kimura et al. 2011).

Each meteorite chip was separately crushed into a fine powder using ceramic mortars and pestles inside a positive pressure ISO 5 HEPA filtered laminar flow hood. A portion of each powdered sample (mass ~0.14–0.36 g, Table 1) was flame-sealed separately in a glass ampoule with 1 ml of ultrapure water and extracted at 100 °C for 24 h (hereafter referred to as "Hot Water [HW] extraction"). Following HW extraction, the supernatants were separated from the residues and half of the HW extract supernatants were subjected to a 6 M ddHCl vapor hydrolysis procedure at 150 °C for 3 h to determine total hydrolyzable amino acid content (Glavin et al. 2006). The acid hydrolyzed HW extracts were then dried under vacuum to remove excess HCl. The residues that remained after completing the HW extraction were then subjected to a second extraction procedure using 6 M ddHCl at 105 °C for 24 h (hereafter referred to as "HCl extraction"). The HCl extraction supernatants were then dried to a residue and set aside until further processing.

Once the supernatants from both extraction procedures were dried to a residue, each residue was individually reconstituted in 1 mL of ultrapure water before being desalted using cation-exchange chromatography. The reconstituted HW and HCl extracts were individually loaded onto separate AG 50W-X8, 100–200 mesh, hydrogen form cation-exchange chromatography columns and desalted as described in

Table 1. Meteorite samples analyzed in this study.

Meteorite[a]	Petrographic type	Subtype (petrology)	Subtype (phyllosilicate fraction)[b]	Subtype (H in OH/H_2O)[c]	Mass extracted (mg)	Fragment (specific, parent)
Y-791198	CM2	2.4[d]	1.6	1.5	138.9	
A-881458	CM2, very weakly heated[e]	—	—	—	176.4	
LEW 90500	CM2	2.4[f]	1.4	1.6	364.4	89, 2
LON 94101	CM2	2.6[f]	1.3	1.8	274.0	101, 8
ALH 83100	CM1/2	2.1[f]	1.2	1.1	280.4	302, 279
MIL 07525	CR2[g]	2.8[h]	—	—	273.1	17, 0
LAP 02342	CR2	2.8[h]	2.7	2.5	298.1	64, 0
MET 00426	CR2	2.8[h]	2.6	2.6	327.3	78, 0
GRO 95577	CR1	2.0[h]	1.3	1.3	342.1	9, 0

[a]Abbreviations: A- = Asuka; Y- = Yamato; LEW = Lewis Cliffs; LON = Lonewolf Nunataks; ALH = Allan Hills; MIL = Miller Range; MET = Meteorite Hills; LAP = La Paz Icefield; GRO = Grosvenor Mountains.
[b]After Howard et al. (2015).
[c]After Alexander et al. (2013).
[d]After Rubin et al. (2007).
[e]After Nakamura (2005) and Kimura et al. (2011).
[f]Estimated using correlations between petrologic type and bulk H and N isotopes from Alexander et al. (2013).
[g]Although Antarctic Meteorite Newsletter, 34 and NASA Antarctic Meteorite Petrographic Description (https://curator.jsc.nasa.gov/antmet/samples/petdes.cfm?sample=MIL07525, accessed on 4/22/2021) classified MIL 07525 as a CR3, subsequent reporting (e.g., Vollmer et al. 2020) has regarded MIL 07525 as a CR2 because of abundant secondary phases.
[h]After Harju et al. (2014).

Simkus et al. (2019). The resultant desalted HW and HCl extract eluates were dried and reconstituted in 100 μL of ultrapure water. Next, 30 μL of each resuspended meteorite extract and the HAA standard solution were separately spiked with 10 μL of the internal standard (8-AOA) before being dried and derivatized for HAA analyses using the following protocol: (1) esterification with 160 μL of isopropanol and 40 μL of acetyl chloride at 100 °C for 3 h, (2) acylation with 50 μL of HFBA at 100 °C for 3 h, (3) removal of excess heptafluorobutyric acids using a stream of dry nitrogen, and (4) dissolution into 10 μL of chloroform before injection into the GC-MS system for analysis. Procedural blanks composed of ultrapure water were prepared in parallel using the identical extraction and processing protocols as the meteorite samples were subjected to, and the procedural blanks were analyzed to provide background-corrected abundance estimates of target analytes.

GC-MS Analysis

The HW and HCl extracts of the CM and CR chondrites were analyzed for HAA abundances, distributions, and enantiomeric ratios by GC-MS. The HFBA-isopropyl derivatives of HAAs were analyzed using a Thermo Trace GC and Thermo DSQII electron-impact quadrupole mass spectrometer. Chromatographic separation was achieved using a 5 m base-deactivated fused silica guard column (Restek) in series with two 25 m CP-Chirasil-Dex CB columns (Agilent), followed by two 25 m Chirasil L-Val columns (Agilent). A helium flow rate of 2.6 mL min^{-1}, and the following temperature program was employed during chromatographic separation: initial oven temperature was 60 °C and was held for 2 min, followed by ramping at 20 °C min^{-1} to 75 °C and held for 40 min, followed by ramping at 20 °C min^{-1} to 120 °C, followed by ramping at 1 °C min^{-1} to 130 °C, and finally ramping at 3 °C min^{-1} to 200 °C and held for 2 min.

The use of two optically active stationary phases in series order of CP-Chirasil-Dex CB and Chirasil L-Val (each 50 m length) is a significant improvement of the GC-MS method used in this study to achieve chromatographic separations of structural isomers and enantiomers of HAAs, compared to previous work (Koga and Naraoka 2017). Other significant improvements include optimization of the derivatization conditions (reagents, reaction temperatures, and durations) and the GC heating program. Furthermore, the GC-MS method was optimized to separate the enantiomers of α-methylserine, an amino acid with the same α-dialkyl structure as isovaline, which has been observed to possess L-enantiomeric excesses in other meteorites (Elsila et al. [2016] and references therein). HAAs in carbonaceous chondrites were identified based

on retention times and mass fragmentation patterns compared to those of commercial standards. To improve instrumental detection limits, we operated the mass spectrometer in single ion monitoring mode to observe the characteristic HAA fragment ions for each analyte. Quantification was performed using the fragment ions of a given analyte that did not experience coelution with potentially interfering ions when analyzing a given sample. This approach helped to improve the accuracy of the quantified measurements reported here. Hence, depending on the presence of interfering ions, in many cases, different fragment ions were used to quantify the same HAAs in different meteorite samples (e.g., m/z 252 and m/z 466 for D,L-α-methylisoserine). A detailed overview of which fragment ions were selected for quantifying a given analyte in each sample is provided in Table S1 in supporting information. HAAs were quantified by comparing the procedural blank-subtracted mass chromatographic peak areas in the meteorite samples to those in the analytical standard analyzed on the same day. The HAA peak areas obtained from the meteorite samples, blanks, and standards were corrected based on the associated peak area of the 8-aminooctanoic acid internal standard in an effort to minimize analytical errors between GC-MS analyses that were executed using different injection volumes (typical injection volumes ranged from 1 to 3 μL).

RESULTS AND DISCUSSION

The Analytical Performance of the Developed Method

Figures 2 and 3 show the extracted ion chromatograms of the HAA derivatives obtained from the HW and HCl extracts of each meteorite, the procedural blanks, and an HAA standard. Most target chiral HAAs were enantiomerically resolved by this GC-MS method, except for α-methylisoserine and β-homoserine (Figs. 2 and 3). Although some chromatographic resolution was achieved for D,L-isoserine, these peaks were not baseline-resolved. The enantiomers of isothreonine and *allo*-isothreonine were successfully separated by the developed method; however, the elution orders of the enantiomers for these species were not determined due to the lack of enantiopure standards.

Although chromatographic resolution of HAA structural isomers was achieved among the analytes in the HAA standard, selected instances of coelution were observed between target HAA species and non-targeted, non-HAA species in some meteorites due to the chemical complexities of the samples studied here. Non-proteinogenic C_4 HAAs were not detected in the procedural blank; however, trace quantities of the common biological contaminants, L-serine and L-threonine, were identified in the procedural blank. The abundances of L-serine and L-threonine in the procedural blank were subtracted when performing quantification analyses of these species in the meteorite extracts. Many of the targeted C_3 and C_4 HAAs were detected in both the HW and HCl extracts, including α-methylisoserine, which had not previously been identified in meteorites due to the lack of a commercially available standard (Koga and Naraoka 2017).

HAA Abundances

The distributions and abundances of HAAs observed in the HW and HCl extracts of the CM chondrites are shown in Table 2. The total HAA content in each extract of the CM chondrites ranged from 2.43 ± 0.09 nmol g^{-1} in the HCl extract of ALH 83100 (CM1/2) to 74 ± 5 nmol g^{-1} in the HCl extract of Y-791198 (CM2). The trend of combined HAA abundances in the two extracts (HW + HCl extracts) of CM chondrites follows the order of Y-791198 (CM2), 126 ± 5 nmol g^{-1} > A-881458 (CM2), 15.2 ± 0.3 nmol g^{-1} > ALH 83100 (CM1/2), 9.8 ± 0.2 nmol g^{-1} > LON 94101 (CM2), 7.0 ± 0.5 nmol $g^{-1} \approx$ LEW 90500 (CM2), 6.94 ± 0.09 nmol g^{-1}. It must be noted that the HW extract of ALH 83100 contained elevated abundances of L-serine (5.0 ± 0.2 nmol g^{-1}) and L-threonine (1.66 ± 0.06 nmol g^{-1}) relative to the total HAA abundances (7.4 ± 0.2 nmol g^{-1}). Consequently, the HW extract of ALH 83100 likely contained significant terrestrial contamination of L-serine and L-threonine. A similar L-serine contamination was observed for the HCl extract of LON 94101 (L-serine: 2.1 ± 0.5 nmol g^{-1}, total abundance: 4.5 ± 0.5 nmol g^{-1}). If these likely L-contaminants are excluded from the total HAA sum, the observed trend in total HAA abundances would appear to be correlated with the phyllosilicate fraction subtype of the CM chondrites (Howard et al. 2015; i.e., CM1.6 Y-791198 > CM1.4 LEW 90500 > CM1.3 LON 94101 > CM1.2 ALH 83100 [Table 1], not included in this trend is A-881458 because this meteorite was not investigated in Howard et al. [2015]).

For the CR chondrites, total HAA content in each extract ranged from 0.42 ± 0.01 nmol g^{-1} for the HW extract of GRO 95577 (CR1) to 171 ± 1 nmol g^{-1} for the HW extract of MIL 07525 (CR2) (Table 3). The trend of combined HAA abundances in the two extracts (HW + HCl extracts) of CR chondrites followed the order of MIL 07525 (CR2), 315 ± 6 nmol g^{-1} > MET 00426 (CR2), 270 ± 10 nmol g^{-1} > LAP 02342 (CR2), 200 ± 10 nmol g^{-1} > GRO 95577 (CR1), 10 ± 1 nmol g^{-1}. This trend is generally correlated with the subtype based on the degree of hydration (wt% H in

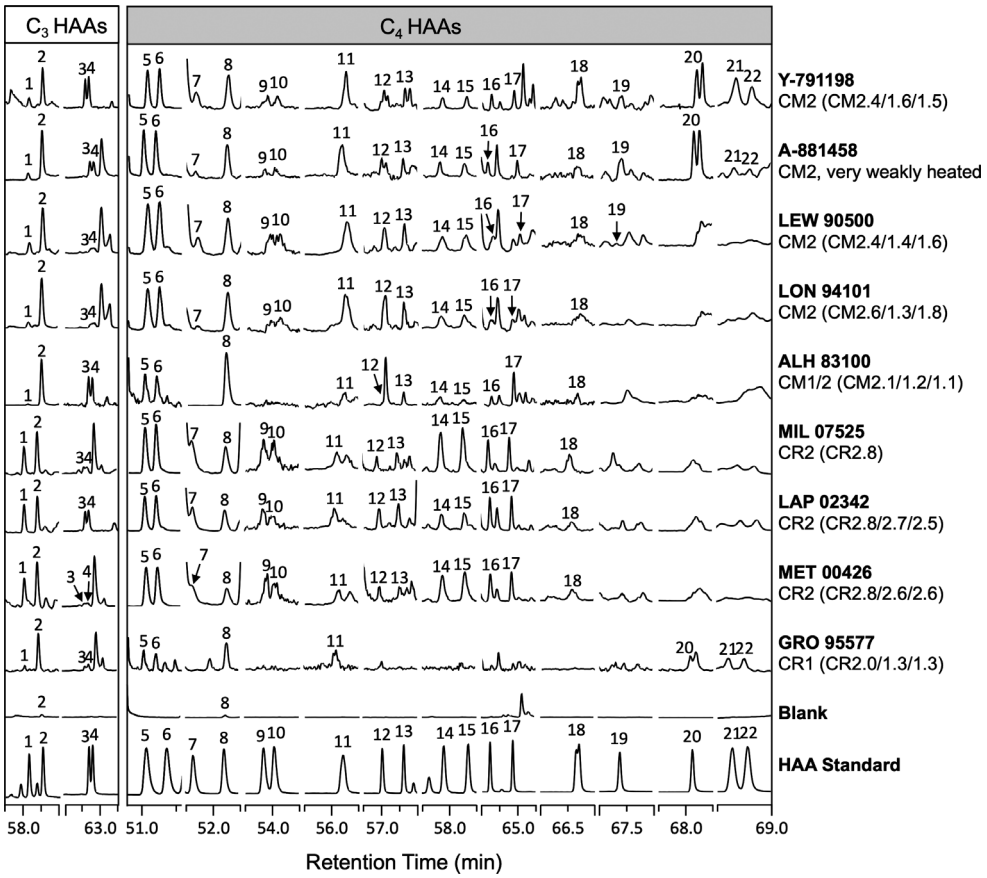

Fig. 2. The selected regions of the GC-MS extracted ion chromatograms of the C_3 and C_4 hydroxy amino acids in the HW extracts of the CM and CR chondrites studied here. Peak identifications are as follows: 57.5–59.0 min for (1) D-serine and (2) L-serine; 62.0–63.5 min for (3) D-isoserine and (4) L-isoserine; 50.6–51.6 min for (5) L-α-methylserine and (6) D-α-methylserine; 51.5–52.5 min for (7) D-threonine and (8) L-threonine; 53.5–54.5 min for (9) D- or L-isothreonine and (10) D- or L-isothreonine; 55.5–56.5 min for (11) DL-α-methylisoserine; 56.5–58.0 min for (12) D-*allo*-threonine and (13) L-*allo*-threonine; 57.5–58.5 min for (14) D- or L-*allo*-isothreonine and (15) D- or L-*allo*-isothreonine; 64.0–65.5 min for (16) D-homoserine and (17) L-homoserine; 66.0–67.0 min for (18) DL-β-homoserine; 67.0–68.0 min for (19) D-3-A-2-HMPA; 67.5–68.5 min for (20) L-4-A-2-HBA; and 68.5–69.0 min for (21) D-4-A-3-HBA and (22) L-4-A-3-HBA. The fragment ions used to generate each chromatogram shown here are detailed in Table S1.

water and OH) of the CR carbonaceous chondrites (Alexander et al. 2013; i.e., CR2.6 MET 00426 > CR 2.5 LAP 02342 > CR1.3 GRO 95577 [Table 1], not included in this trend is MIL 07525, which was not investigated by Alexander et al. [2013]).

Interestingly, the CR2 chondrites (MIL 07525, LAP 02342, and MET 00426) contained greater abundances of the individual HAAs, serine and α-methylserine, when summed from their respective HW + HCl extracts, than any other α-HAA detected in the summed HW + HCl extracts of any of the CM or CR meteorites (Table 4). The total abundances of α-HAAs were higher in the CR2 chondrites compared to the CM2 chondrites. In contrast to this disparity among α-HAAs, the abundances of β- and γ-HAAs in CR chondrites were within a similar range to those in CM chondrites. For example, the combined β-HAA abundances in the two extracts of each CR chondrite ranged from 0.82 ± 0.01 nmol g^{-1} for GRO 95577 to 18.4 ± 0.6 nmol g^{-1} for MIL 07525, while those of CM chondrites ranged from 0.69 ± 0.02 nmol g^{-1} for ALH 83100 to 37.1 ± 0.9 nmol g^{-1} for Y-791198. Likewise, the combined γ-HAA abundances in the two extracts of each CR chondrite ranged from 0.112 ± 0.005 nmol g^{-1} for GRO 95577 to 1.3 ± 0.1 nmol g^{-1} for MIL 07525, while those of CM chondrites ranged from 0.098 ± 0.002 nmol g^{-1} for ALH 83100 to 3.14 ± 0.09 nmol g^{-1} for Y-791198. This marks the first reporting of disparities between total abundances of α-HAAs compared to β- and γ-HAAs in CM and CR chondrites, possibly indicating that varying formation pathways may be responsible for the observed differences.

It is also worth noting that for all CR2 meteorites and most of the CMs studied here, the HCl extracts are

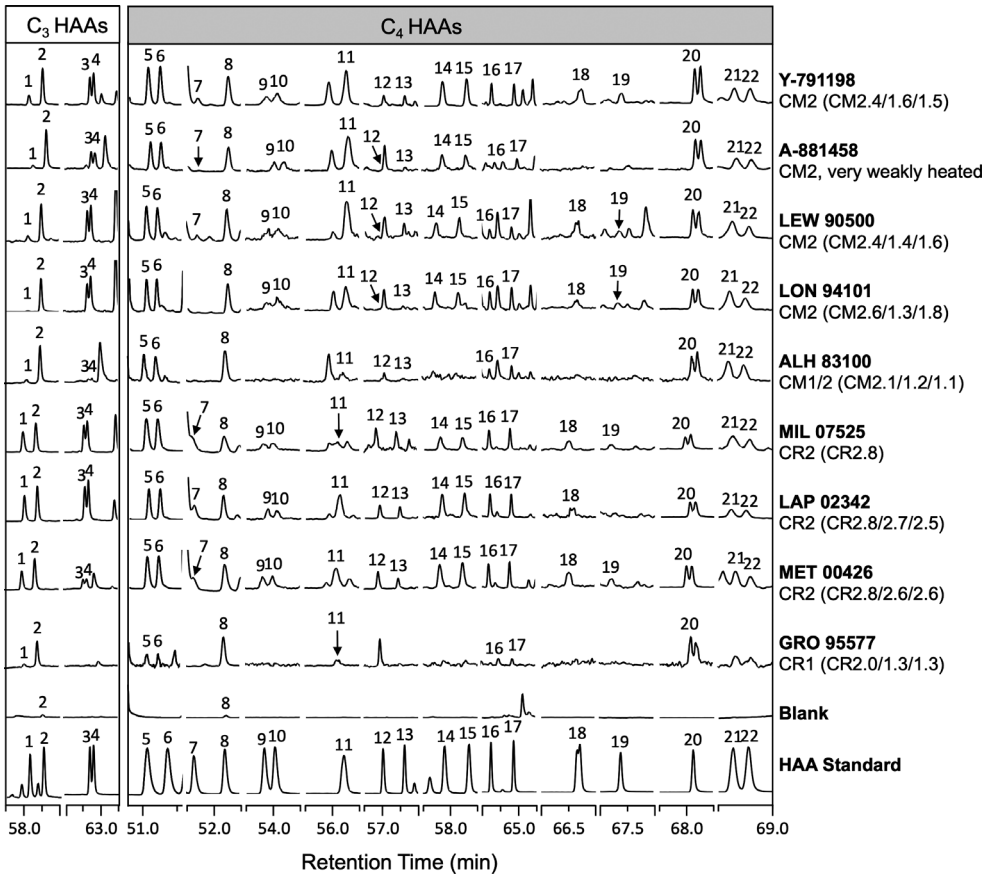

Fig. 3. The selected regions of the GC-MS extracted ion chromatograms of the C_3 and C_4 hydroxy amino acids in the 6 M HCl extracts of the CM and CR chondrites studied here. Peak identifications are the same as in Fig. 2. The fragment ions used to generate each chromatogram shown here are detailed in Table S1.

the only ones that contain γ-HAAs (Tables 2 and 3). It is possible that an exposure of γ-HAA precursors in the meteorite matrix to HCl during the extraction process might induce the formation or liberation of γ-HAAs, or their precursors to allow synthesis during workup. Further work is needed to investigate whether a discrepancy among structural amino acid isomer distributions between HW and HCl extracts would also be observed for conventional amino acids (e.g., C_5 amino acid isomers, as investigated in previous works [Elsila et al. 2016] and references therein).

Figures 4A and 4B show the relative abundances of C_3 and C_4 HAAs in the HW and HCl extracts, respectively, as a function of amine position (α-, β-, or γ-) relative to the total abundance of C_3 and C_4 HAAs. The relative abundances were calculated from the data in Tables 2 and 3. The relative abundances of α-HAAs were larger than those of β-HAAs and γ-HAAs for the HW and HCl extracts of all CM and CR chondrites (Figs. 4A and 4B). It must be noted that the relative abundances in the HW extract of ALH 83100 and the HCl extract of GRO 95577 were biased toward α-HAA isomers by relatively significant L-serine and L-threonine abundances that were likely due to terrestrial contamination (see Tables 2 and 3). For each meteorite, the relative abundance of β-HAAs in the HCl extract was comparable to, or greater than, that in the respective HW extract, except for LON 94101 and GRO 95577 (Figs. 4A and 4B). Similarly, the relative abundances of γ-HAAs in the HCl extract of each meteorite were comparable to, or greater than, that in the respective HW extract, except for GRO 95577. The observed difference in relative abundances between the HW extract of CR1 GRO 95577 and all the other extracts of all the other CRs studied here is intriguing. Further work is needed to determine the origins of this difference, but that is beyond the scope of the present study.

Figure 4C shows the relative HAA abundances in the combined (HW + HCl) extracts of CM and CR chondrites as a function of amine position (α-, β-, or γ-). The α-HAA isomers dominate the distribution of

Table 2. Summary of the average abundances (nmol g^{-1}) of the three- to four-carbon hydroxy amino acids identified in the HW and HCl extracts of CM carbonaceous chondrites measured by GC-MS.[a]

Hydroxy amino acids (amine position)	Y-791198		A-881458		LEW 90500		LON 94101		ALH 83100	
	CM1/2		CM1/2		CM1/2		CM1/2		CM1/2	
	Hot water	HCl	Hot water	HCl	Hot water	HCl	Hot water	HCl	Hot water	HCl
D-Serine (α)	4.2[b]	7 ± 2	0.29 ± 0.01	0.67 ± 0.03	0.088 ± 0.007	0.137 ± 0.005	0.12 ± 0.02	0.26 ± 0.05	0.16 ± 0.01	0.14 ± 0.01
L-Serine (α)	9.5[b]	18 ± 4	2.2 ± 0.2	1.60 ± 0.07	0.24 ± 0.03	0.69 ± 0.07	0.7 ± 0.1	2.1 ± 0.5	5.0 ± 0.2	1.05 ± 0.09
DL-Isoserinee (β)	1.40 ± 0.03	8.2 ± 0.4	0.53 ± 0.02	0.46 ± 0.03	0.44 ± 0.02	0.149 ± 0.006	0.369 ± 0.008	0.125 ± 0.009	0.133 ± 0.004	0.41 ± 0.01
L-α-Methylserine (α)	12 ± 1	7.8 ± 0.5	1.13 ± 0.07	0.366 ± 0.009	0.749 ± 0.009	0.133 ± 0.001	0.272 ± 0.003	0.20 ± 0.03	0.034 ± 0.002	0.126 ± 0.004
D-α-Methylserine (α)	13 ± 1	7.9 ± 0.5	1.2 ± 0.1	0.38 ± 0.01	0.76 ± 0.01	0.127 ± 0.002	0.261 ± 0.001	0.19 ± 0.02	0.0347 ± 0.0005	0.120 ± 0.006
D-Threonine (α)	0.40[d] ± 0.07	0.35[d] ± 0.05	0.033 ± 0.004	0.019 ± 0.007	0.061[d] ± 0.002	0.0140 ± 0.0002	0.013 ± 0.001	0.013 ± 0.001	n.d.	n.d.
L-Threonine (α)	0.6 ± 0.1	1.2 ± 0.2	0.22 ± 0.01	0.75 ± 0.04	0.106 ± 0.004	0.077 ± 0.002	0.124 ± 0.003	0.41 ± 0.05	1.66 ± 0.06	0.35 ± 0.01
D-*allo*-Threonine (α)	0.14[d] ± 0.02	0.22 ± 0.02	0.034[d] ± 0.003	0.017[d]	0.059[d] ± 0.003	0.012[d]	0.018[d]	0.017[d]	0.054[d]	0.013[d]
L-*allo*-Threonine (α)	0.19[d] ± 0.04	0.22 ± 0.02	0.036[d] ± 0.003	0.017 ± 0.003	0.050 ± 0.004	0.012 ± 0.001	0.018 ± 0.002	0.017[d] ± 0.001	0.054 ± 0.004	0.013 ± 0.001
D-Homoserine (α)	0.62[d] ± 0.07	0.99[d] ± 0.04	0.35 ± 0.02	0.063 ± 0.006	0.084[d]	0.079 ± 0.005	0.040[d] ± 0.002	0.067 ± 0.009	0.033 ± 0.001	0.0249 ± 0.0005
L-Homoserine (α)	0.61 ± 0.07	0.97 ± 0.04	0.37 ± 0.01	0.084[d] ± 0.001	0.084[d] ± 0.005	0.079 ± 0.003	0.038[d] ± 0.001	0.08 ± 0.01	0.105 ± 0.002	0.0293 ± 0.0008
DL-α-Msethylisoserine[e] (β)	5.4 ± 0.2	14.6 ± 0.8	0.86 ± 0.07	1.91 ± 0.09	0.97 ± 0.02	0.85 ± 0.01	0.33 ± 0.02	0.57[d] ± 0.02	0.045 ± 0.006	0.060 ± 0.006
DL-Isothreonine[f] (β)	0.6 ± 0.1	1.8 ± 0.2	0.18 ± 0.03	0.119 ± 0.006	0.23 ± 0.01	0.087 ± 0.007	0.09 ± 0.02	0.08 ± 0.01	n.d.	n.d.
DL-*allo*-Isothreonine[f] (β)	0.50 ± 0.03	1.11 ± 0.04	0.095 ± 0.007	0.089 ± 0.006	0.122 ± 0.006	0.048 ± 0.001	0.086 ± 0.006	0.041 ± 0.005	0.019 ± 0.002	n.d.
DL-β-Homoserine[e] (β)	0.98 ± 0.04	0.72 ± 0.03	0.073 ± 0.007	n.d.	0.064 ± 0.002	0.079 ± 0.004	0.08 ± 0.01	0.074 ± 0.002	0.025 ± 0.002	n.d.
D-3-A-2-HMPA[g] (γ)	1.0[d] ± 0.1	0.7 ± 0.1	0.131[d] ± 0.008	0.11 ± 0.02	n.d.	0.027[d] ± 0.002	n.d.	0.034[d] ± 0.002	n.d.	n.d.
L-4-A-2-HBA[g] (γ)	0.78[d] ± 0.04	1.52 ± 0.08	0.28 ± 0.01	0.24 ± 0.04	n.d.	0.093 ± 0.003	n.d.	0.072 ± 0.008	n.d.	0.038 ± 0.001
D-4-A-3-HBA (γ)	0.352[d] ± 0.002	0.121 ± 0.005	0.056[d] ± 0.006	0.08[d] ± 0.01	n.d.	0.084[d] ± 0.001	n.d.	0.062[d] ± 0.003	n.d.	0.036[d] ± 0.002
L-4-A-3-HBA (γ)	0.23 ± 0.01	0.132 ± 0.007	0.042 ± 0.005	0.06 ± 0.01	n.d.	0.044 ± 0.002	n.d.	0.031 ± 0.002	n.d.	0.0243 ± 0.0008
Total (nmol g^{-1})	52 ± 2[g]	74 ± 5	8.1 ± 0.3	7.0 ± 0.1[g]	4.12 ± 0.05[g]	2.8 ± 0.1[g]	2.5 ± 0.1[g]	4.5 ± 0.5[g]	7.4 ± 0.2[g]	2.43 ± 0.09[g]
Sum of HW & HCl (nmol g^{-1})	126 ± 5[g]		15.2 ± 0.3[g]		6.94 ± 0.09[g]		7.0 ± 0.5[g]		9.8 ± 0.2[g]	
HW/(HW + HCl)	41%		54%		59%		36%		75%	

The gray shadings were used to distinguish each hydroxy amino acid isomer with the D- and L-enantiomer (e.g., D- and L-serine is white, DL-isoserine is gray, L- and D-α-methylserine is white, and so on). n.d. = value not determined due to trace amino acid abundances.

[a]Sample extracts were analyzed by HFBA-isopropyl derivatization and GC-MS. The reported uncertainties (δx) are based on the standard deviation value (σx) of 2-3 separate measurements (n) with a standard error, $\delta x = \sigma x \times (n)^{-1/2}$.

[b]Minimum abundances are shown without an accompanying standard error because replicate measurements of this analyte were not made.

[c]The enantiomers were not resolved by the chromatographic separation applied in this study.

[d]The abundances and their associated uncertainties presented here are approximate due to quantitative interferences posed by coeluting species (e.g., non-HAA species or D-α-methylserine coeluting with D-threonine) in the meteorite sample.

[e]The abundances were reported as the combined quantity estimates of both enantiomers because although the enantiomers were separated, the elution orders of the respective enantiomers were not determined due to a lack of enantiopure standard availability.

[f]Precise abundance estimates are not provided due to the lack of enantiopure standards. Instead, upper limit abundances were estimated.

[g]Total abundances were determined using individual HAA abundance estimates that were not accompanied by a standard error, which may cause the true uncertainties of the total abundance estimates to be larger than the total uncertainty estimates provided here.

Table 3. Summary of the average abundances (nmol g^{-1}) of the three- to four-carbon hydroxy amino acids identified in the HW and HCl extracts of CR carbonaceous chondrites measured by GC-MS.[a]

Hydroxy amino acids (Amine position)	MIL 07525		LAP 02342		MET 00426		GRO 95577	
	CR2		CR2		CR2		CR1	
	Hot water	HCl	Hot water	HCl	Hot water	HCl	Hot water	HCl
D-Serine (α)	11[b]	25[b]	1.9 ± 0.2	51 ± 7	23 ± 8	38 ± 1	0.0166 ± 0.0005	1.3 ± 0.2
L-Serine (α)	12[b]	27[b]	2.1 ± 0.2	52 ± 7	23 ± 10	46 ± 1	0.13 ± 0.01	6 ± 1
DL-Isoserine[e] (β)	1.44 ± 0.09	5.5 ± 0.5	0.43 ± 0.03	1.2 ± 0.1	0.98 ± 0.07	3.1 ± 0.1	0.085 ± 0.005	0.075 ± 0.004
L-α-Methylserine (α)	60.9 ± 0.7	34 ± 4	20 ± 2	14 ± 2	24 ± 1	29.5 ± 0.2	0.0154 ± 0.0003	0.051 ± 0.004
D-α-Methylserine (α)	67.9 ± 0.6	38 ± 4	23 ± 2	14 ± 2	26 ± 2	33.6 ± 0.4	0.014 ± 0.001	0.051 ± 0.001
D-Threonine (α)	2.78[d] ± 0.04	1.4[d] ± 0.2	1.3[d] ± 0.1	1.1[d] ± 0.2	0.047[d] ± 0.02	1.6[d] ± 0.1	n.d.	n.d.
L-Threonine (α)	2.68 ± 0.05	1.8 ± 0.2	1.2 ± 0.1	1.4[d] ± 0.3	0.84 ± 0.06	3.73 ± 0.06	0.040 ± 0.006	1.3 ± 0.3
D-*allo*-Threonine (α)	1.81 ± 0.05	0.8 ± 0.1	2.1[d] ± 0.8	0.5 ± 0.1	0.7[d] ± 0.1	1.22 ± 0.04	n.d.	n.d.
L-*allo*-Threonine (α)	2.42[d] ± 0.09	0.7 ± 0.1	2.2[d] ± 0.8	0.45 ± 0.08	0.80[d] ± 0.03	1.32[d] ± 0.04	n.d.	n.d.
D-Homoserine (α)	1.33[d] ± 0.08	1.5[d] ± 0.1	0.54[d] ± 0.03	0.48[d] ± 0.03	1.46[d] ± 0.08	1.02 ± 0.04	0.0049[d] ± 0.0005	0.022[d] ± 0.002
L-Homoserine (α)	1.16 ± 0.08	1.5[d] ± 0.1	0.49 ± 0.02	0.45 ± 0.03	1.36 ± 0.09	0.98 ± 0.05	0.0042[d] ± 0.0003	0.0475[d] ± 0.0007
DL-α-Methylisoserine[e] (β)	2.8 ± 0.1	1.9[d] ± 0.2	0.33 ± 0.04	10 ± 2	1.3 ± 0.1	4.0 ± 0.1	0.047 ± 0.003	0.61 ± 0.01
DL-Isothreonine[f] (β)	1.7 ± 0.1	2.1 ± 0.2	0.272 ± 0.002	0.54 ± 0.06	0.68 ± 0.03	2.42 ± 0.09	n.d.	n.d.
D*L-allo*-Isothreonine[f] (β)	0.87 ± 0.02	0.85 ± 0.08	0.084[d] ± 0.004	0.16 ± 0.01	0.306 ± 0.008	0.68 ± 0.01	n.d.	n.d.
DL-β-Homoserine[e] (β)	0.51 ± 0.04	0.55 ± 0.04	0.098 ± 0.003	0.119 ± 0.009	0.40 ± 0.03	0.259 ± 0.006	n.d.	n.d.
D-3-A-2-HMPA[g] (β)	n.d.	0.26[d] ± 0.02	n.d.	0.0102[d] ± 0.002	n.d.	0.082 ± 0.003	n.d.	n.d.
D-4-A-2-HBA[g] (γ)	n.d.	0.8 ± 0.1	n.d.	0.38 ± 0.01	n.d.	0.37 ± 0.02	0.041 ± 0.003	0.040 ± 0.003
D-4-A-3-HBA (γ)	n.d.	0.34[d] ± 0.03	n.d.	0.15[d] ± 0.01	n.d.	0.090[d] ± 0.003	0.017[d] ± 0.001	n.d.
L-4-A-3-HBA (γ)	n.d.	0.20 ± 0.03	n.d.	0.12 ± 0.01	n.d.	0.073 ± 0.004	0.013 ± 0.002	n.d.
Total (nmol g^{-1})	171 ± 1[g]	144 ± 6[g]	56 ± 3	148 ± 10	110 ± 10	168 ± 2	0.42 ± 0.01	10 ± 1
Sum of HW & HCl (nmol g^{-1})	315 ± 6[g]		200 ± 10		270 ± 10		10 ± 1	
HW/(HW + HCl) (%)	54		27		39		4	

The gray shadings were used to distinguish each hydroxy amino acid isomer with the D- and L-enantiomer (e.g., D- and L-serine is white, DL-isoserine is gray, L- and D-α-methylserine is white, and so on). n.d. = value not determined due to trace amino acid abundances.

[a]Sample extracts were analyzed by HFBA-isopropyl derivatization and GC-MS. The reported uncertainties (δx) are based on the standard deviation value (σx) of 2-3 separate measurements (n) with a standard error, $\delta x = \sigma x \times (n)^{-1/2}$.

[b]Minimum abundances are shown without an accompanying standard error because replicate measurements of this analyte were not made.

[c]The enantiomers were not resolved by the chromatographic separation applied in this study.

[d]The abundances and their associated uncertainties presented here are approximate due to quantitative interferences posed by coeluting species (e.g., non-HAA species or D-α-methylserine coeluting with D-threonine) in the meteorite sample.

[e]The abundances were reported as the combined quantity estimates of both enantiomers because although the enantiomers were separated, the elution orders of the respective enantiomers were not determined due to a lack of enantiopure standard availability.

[f]Precise abundance estimates are not provided due to the lack of enantiopure standards. Instead, upper limit abundances were estimated.

[g]Total abundances were determined using individual HAA abundance estimates that were not accompanied by a standard error, which may cause the true uncertainties of the total abundance estimates to be larger than the total uncertainty estimates provided here.

Table 4. Summary of the combined abundances (nmol g^{-1}) of the three- to four-carbon hydroxy amino acids in the two extracts (HW + HCl extracts) of CM and CR carbonaceous chondrites measured by GC-MS.[a]

	Y-791198	A-881458	LEW 90500	LON 94101	ALH 83100	MIL 07525	LAP 02342	MET 00426	GRO 95577
Hydroxy amino acids	CM2	CM2	CM2	CM2	CM1/2	CR2	CR2	CR2	CR1
(Amine position)	HW + HCl	HW + HCl	HW + HCl	HW + HCl	HW + HCl	HW + HCl	HW + HCl	HW + HCl	HW + HCl
D-Serine (α)	11 ± 2[b]	0.97 ± 0.04	0.225 ± 0.009	0.37 ± 0.05	0.30 ± 0.02	36[c]	53 ± 7	62 ± 8	1.3 ± 0.2
L-Serine (α)	28 ± 4[b]	3.8 ± 0.3	0.94 ± 0.07	2.8 ± 0.5	6.1 ± 0.2	39[c]	54 ± 7	69 ± 10	6 ± 1
DL-Isoserine[e] (β)	9.6 ± 0.4	0.99 ± 0.03	0.59 ± 0.02	0.49 ± 0.01	0.54 ± 0.01	6.9 ± 0.5	1.6 ± 0.1	4.1 ± 0.1	0.160 ± 0.006
L-α-Methylserine (α)	20 ± 1	1.50 ± 0.07	0.882 ± 0.009	0.47 ± 0.03	0.160 ± 0.004	95 ± 4	33 ± 3	53 ± 1	0.067 ± 0.004
D-α-Methylserine (α)	21 ± 1	1.5 ± 0.1	0.89 ± 0.01	0.45 ± 0.02	0.155 ± 0.006	106 ± 4	38 ± 3	60 ± 2	0.066 ± 0.002
D-Threonine (α)	0.75[e] ± 0.09	0.052 ± 0.008	0.075[e] ± 0.002	0.026 ± 0.002	n.d.	4.2[e] ± 0.2	2.3[e] ± 0.2	2.1[e] ± 0.1	n.d.
L-Threonine (α)	1.8 ± 0.2	0.97 ± 0.04	0.183 ± 0.004	0.54 ± 0.05	2.01 ± 0.06	4.5 ± 0.2	2.6[e] ± 0.3	4.58 ± 0.08	1.3 ± 0.3
D-*allo*-Threonine (α)	0.36[e] ± 0.02	0.052[e] ± 0.005	0.071[e] ± 0.003	0.036[e] ± 0.002	0.068[e] ± 0.004	2.6 ± 0.1	2.6[e] ± 0.8	1.9[e] ± 0.1	n.d.
L-*allo*-Threonine (α)	0.41[e] ± 0.04	0.053[e] ± 0.005	0.062 ± 0.004	0.036[e] ± 0.002	0.068 ± 0.004	3.2[e] ± 0.1	2.6[e] ± 0.8	2.12[e] ± 0.05	n.d.
D-Homoserine (α)	1.61[e] ± 0.08	0.41 ± 0.02	0.163[e] ± 0.007	0.107[e] ± 0.009	0.058 ± 0.001	2.8[e] ± 0.2	1.02[e] ± 0.04	2.48[e] ± 0.09	0.027[e] ± 0.002
L-Homoserine (α)	1.58 ± 0.08	0.45[e] ± 0.01	0.163[e] ± 0.006	0.12[e] ± 0.01	0.134 ± 0.002	2.6[e] ± 0.1	0.94 ± 0.04	2.3 ± 0.1	0.0518[e] ± 0.0008
DL-α-Methylisoserine[e] (β)	20.0 ± 0.8	2.8 ± 0.1	1.82 ± 0.03	0.90[e] ± 0.03	0.105 ± 0.008	4.7[e] ± 0.2	10 ± 2	5.3 ± 0.2	0.66 ± 0.01
DL-Isothreonine[f] (β)	2.5 ± 0.2	0.30 ± 0.03	0.32 ± 0.01	0.17 ± 0.02	n.d.	3.7 ± 0.3	0.81 ± 0.06	3.1 ± 0.1	n.d.
DL-*allo*-Isothreonine[f] (β)	1.61 ± 0.05	0.184 ± 0.009	0.170 ± 0.006	0.127 ± 0.007	0.019 ± 0.002	1.72 ± 0.09	0.24[e] ± 0.01	0.99 ± 0.02	n.d.
DL-β-Homoserine[e] (β)	1.69 ± 0.05	0.073 ± 0.007	0.143 ± 0.004	0.16 ± 0.01	0.025 ± 0.002	1.06 ± 0.05	0.217 ± 0.009	0.66 ± 0.03	n.d.
D-3-A-2-HMPA[g] (β)	1.7[e] ± 0.2	0.24[e] ± 0.02	0.027[e] ± 0.002	0.034[e] ± 0.002	n.d.	0.26[e] ± 0.02	0.102[e] ± 0.002	0.082 ± 0.003	n.d.
L-4-A-2-HBA[g] (γ)	2.30[e] ± 0.09	0.52 ± 0.04	0.093 ± 0.003	0.072 ± 0.008	0.038 ± 0.001	0.81 ± 0.07	0.38 ± 0.01	0.37 ± 0.02	0.081 ± 0.005
D-4-A-3-HBA (γ)	0.474[e] ± 0.005	0.13[e] ± 0.01	0.084[e] ± 0.001	0.062[e] ± 0.003	0.036[e] ± 0.002	0.34[e] ± 0.03	0.15[e] ± 0.01	0.090[e] ± 0.003	0.017[e] ± 0.001
L-4-A-3-HBA (γ)	0.37 ± 0.01	0.10 ± 0.01	0.044 ± 0.002	0.031 ± 0.002	0.0243 ± 0.0008	0.20 ± 0.03	0.12 ± 0.01	0.073 ± 0.004	0.013 ± 0.002
Total of α-HAAs	85 ± 5[h]	9.9 ± 0.3[h]	3.65 ± 0.08[h]	4.9 ± 0.5[h]	9.0 ± 0.2[h]	296 ± 6[h]	190 ± 10	260 ± 10	9 ± 1
Total of β-HAAs	37.1 ± 0.9	4.6 ± 0.1	3.07 ± 0.04	1.89 ± 0.04	0.69 ± 0.02	18.4 ± 0.6	13 ± 2	14.2 ± 0.3	0.82 ± 0.01
Total of γ-HAAs	3.14 ± 0.09	0.75 ± 0.04	0.220 ± 0.004	0.164 ± 0.009	0.098 ± 0.002	1.3 ± 0.1	0.65 ± 0.02	0.53 ± 0.02	0.112 ± 0.005
Sum of HW & HCl (nmol g^{-1})	126 ± 5[h]	15.2 ± 0.3[h]	6.94 ± 0.09[h]	7.0 ± 0.5[h]	9.8 ± 0.2[h]	315 ± 6[h]	200 ± 10	270 ± 10	10 ± 1

The gray shadings were used to distinguish each hydroxy amino acid isomer with the D- and L-enantiomer (e.g., D- and L-serine is white, DL-isoserine is gray, L- and D-α-methylserine is white, and so on). n.d. = value not determined due to trace amino acid abundances.

[a]The combined abundances in the HW and HCl extracts were summed from Table 2 and 3, and the uncertainties ($\delta x_{combined}$) were propagated through the relevant equations with $\delta x_{combined} = (\delta x_{HW}^2 + \delta x_{HCl}^2)^{1/2}$.

[b]Combined abundances were determined using individual HAA abundance estimates that were not accompanied by a standard error, which may cause the true uncertainties of the total abundance estimates to be larger than the total uncertainty estimates provided here.

[c]Minimum abundances are shown without an accompanying standard error because replicate measurements of this analyte were not made.

[d]The enantiomers were not resolved by the chromatographic separation applied in this study.

[e]The abundances and their associated uncertainties presented here are approximate due to quantitative interferences posed by coeluting species (e.g., non-HAA species or D-α-methylserine coeluting with D-threonine) in the meteorite sample.

[f]The abundances were reported as the combined quantity estimates of both enantiomers because although the enantiomers were separated, the elution orders of the respective enantiomers were not determined due to a lack of enantiopure standard availability.

[g]Precise abundance estimates are not provided due to the lack of enantiopure standards. Instead, upper limit abundances were estimated.

[h]Total abundances were determined using individual HAA abundance estimates that were not accompanied by a standard error, which may cause the true uncertainties of the total abundance estimates to be larger than the total uncertainty estimates provided here.

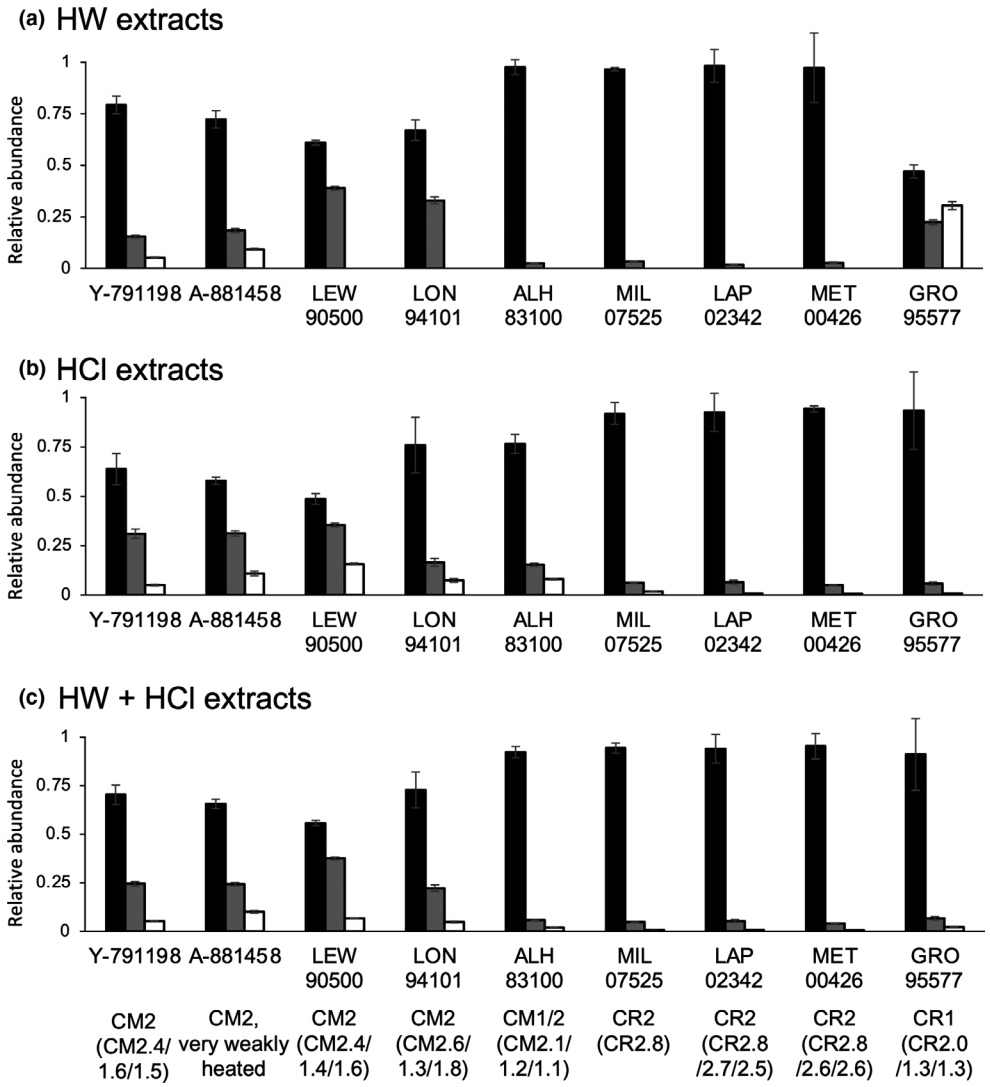

Fig. 4. The relative abundances of C_3 and C_4 hydroxy amino acids in CM and CR carbonaceous chondrites for (A) the HW extracts, (B) the HCl extracts, and (C) the combined (HW + HCl) extracts. Relative abundances are displayed as functions of amine position (α-, β-, γ-) relative to the total abundances of C_3 and C_4 hydroxy amino acids. The relative abundances were calculated from the data in Tables 2 and 3, and the uncertainties were determined by appropriate propagation of the standard errors. In all figure panes, black bars denote α-amines, gray bars denote β-amines, and white bars denote γ-amines.

C_3 and C_4 HAA isomers for all meteorites. In particular, the CR2 chondrites (MIL 07525, LAP 02342, and MET 00426) showed larger relative abundances of α-HAA isomers than β- or γ-HAA isomers, mainly deriving from abundant serine and α-methylserine (see Table 3). In contrast, the CM2 chondrites (Y-791198, A-881458, LEW 90500, and LON 94101) possessed noticeably greater relative abundances of β- and γ-HAAs than the CR chondrites studied here. The disparities between the relative abundances of α-HAAs compared to β- and γ-HAAs in the CM2 and CR chondrites might suggest that different HAA formation, and/or preservation, mechanisms occurred in CM and CR chondrite parent bodies.

Enantiomeric Compositions of Non-Proteinogenic Hydroxy Amino Acids

Since α-dialkyl amino acids, such as isovaline, have been targeted in previous meteorite studies to evaluate their enantiomeric excesses in meteorites, given their resistances to racemization (Pollock et al. 1975), a similar α-dialkyl amino acid, α-methylserine, was targeted in this study to explore its possible enantiomeric excess in meteorites. We first resolved D,L-

α-methylserine in carbonaceous chondrites using the developed GC-MS method (Figs. 2 and 3). However, it was found that α-methylserine was racemic within error in most carbonaceous chondrite extracts (Table 5). Thus, the α-methylserine in CM and CR chondrites did not appear to show convincing L-enantiomeric excesses correlating with the degree of aqueous alteration, a phenomenon observed in isovaline (Elsila et al. [2016] and references therein; Glavin et al. 2020a, 2020b).

The notable exceptions to this observation of racemic α-methylserine included the HCl extracts of LEW 90500 and MET 00426, and the HW extracts of LON 094101 and MIL 07525. These extracts of LEW 90500 and LON 094101 contained very nearly racemic mixtures of α-methylserine that were slightly L-enantiomerically enriched, outside of the measurement error, as they exhibited α-methylserine L-enantiomeric excesses of $2.4 \pm 0.8\%$ and $1.9 \pm 0.6\%$, respectively (Table 5). The aforementioned extracts of MIL 07525 and MET 00426 showed slight D-α-methylserine enantiomeric enrichments outside of errors, as they exhibited α-methylserine L-enantiomeric excesses of $-5.4 \pm 0.8\%$ and $-6.6 \pm 0.8\%$, respectively (Table 5). These narrow L- or D-α-methylserine enantiomeric excesses observed outside of errors are anomalous compared to the α-methylserine data collected from most other meteorite extracts analyzed here. They are also inconsistent with the findings from their respective HW or HCl extract counterparts for the same samples, which showed α-methylserine was racemic. Future quantitative analyses are necessary to determine if these anomalies are similarly observed by alternative analytical methodologies, such as ultraperformance liquid chromatography with fluorescence detection and time-of-flight mass spectrometry (UPLC-FD/ToF-MS; Glavin et al. 2020b).

The other non-proteinogenic α-HAAs, namely *allo*-threonine and homoserine, were affected by coelution with interfering species in most of the carbonaceous chondrites we studied, which made accurate quantification of their enantiomers not possible (Figs. 2 and 3). Some meteorite extracts showed the chromatographic peaks of *allo*-threonine and homoserine without coelution. In these cases, *allo*-threonine and homoserine were racemic within analytical errors, except for homoserine in ALH 83100 (Table 5). The L-enantiomeric excess for homoserine observed in the HW and HCl extracts of ALH 83100 were $51.7 \pm 1.2\%$ and $8.0 \pm 1.6\%$, respectively (Table 5). However, it should be noted that L-homoserine can be produced by methionine metabolism as a terrestrial biological component (Matsuo and Greenberg 1955). Furthermore, in this study, we observed relatively significant abundances of L-serine and L-threonine in both extracts of ALH 83100, which were terrestrial contamination (Table 2). Thus, it is plausible that the L-enantiomeric excesses of homoserine in the HW and HCl extracts of ALH 83100 could also be derived from terrestrial contamination. Future isotopic measurements will be required to determine the origin of the L-homoserine enantiomeric excesses in ALH 83100.

A Proposed Formation Mechanism for Prominent α-Hydroxy Amino Acids: Strecker Cyanohydrin Synthesis

This study revealed that α-methylserine and serine were significantly more abundant in the combined (HW + HCl) extracts of CR2 chondrites (LAP 02342, MET 00426, and MIL 07525) than other α-HAAs, such as threonine, *allo*-threonine, and homoserine (Table 4). These large abundances of serine and α-methylserine may be explained by the predominance of the Strecker cyanohydrin synthesis within the parent bodies of the CR chondrites during the aqueous alteration phase, as has been proposed to explain the presence of other α-amino acids in meteorite samples (Peltzer and Bada 1978; Peltzer et al. 1984; Lerner et al. 1993; Glavin et al. 2010). The predominance of α-methylserine and serine compared to other α-HAAs could be used to make inferences about the relative abundances of α-HAA precursors in CR chondrite parent bodies that could have been more significantly incorporated into the Strecker cyanohydrin synthesis to generate their respective HAAs. In particular, inferences could be made about the potential for elevated relative abundances of possible carbonyl-containing precursors of α-methylserine (hydroxyacetone), serine (glycolaldehyde), threonine and/or *allo*-threonine (lactaldehyde), and homoserine (3-hydroxypropanal), as illustrated in the proposed Strecker cyanohydrin formation mechanisms shown in Fig. 5.

One critical aspect of the Strecker cyanohydrin synthesis that could have also contributed to elevated abundances of α-methylserine and serine in the extracts of the CR2 chondrites studied here is the abundance of ammonia in the CR meteorite parent bodies. It has been reported that CR2 chondrites were enriched in ammonia, and that ammonia was present not only in the free form but also in a bound form that can be released from insoluble organic matter by hydrothermal treatment (Pizzarello and Holmes 2009; Pizzarello et al. 2011). This finding suggests that parent body environments of CR2 chondrites may have contained elevated abundances of ammonia. In such ammonia-enriched environments, the Strecker cyanohydrin synthesis (see Fig. 5 for examples) could have proceeded by forming an imine from a precursor aldehyde or ketone, in the presence of ammonia. The imine could then react with HCN to form an aminonitrile that

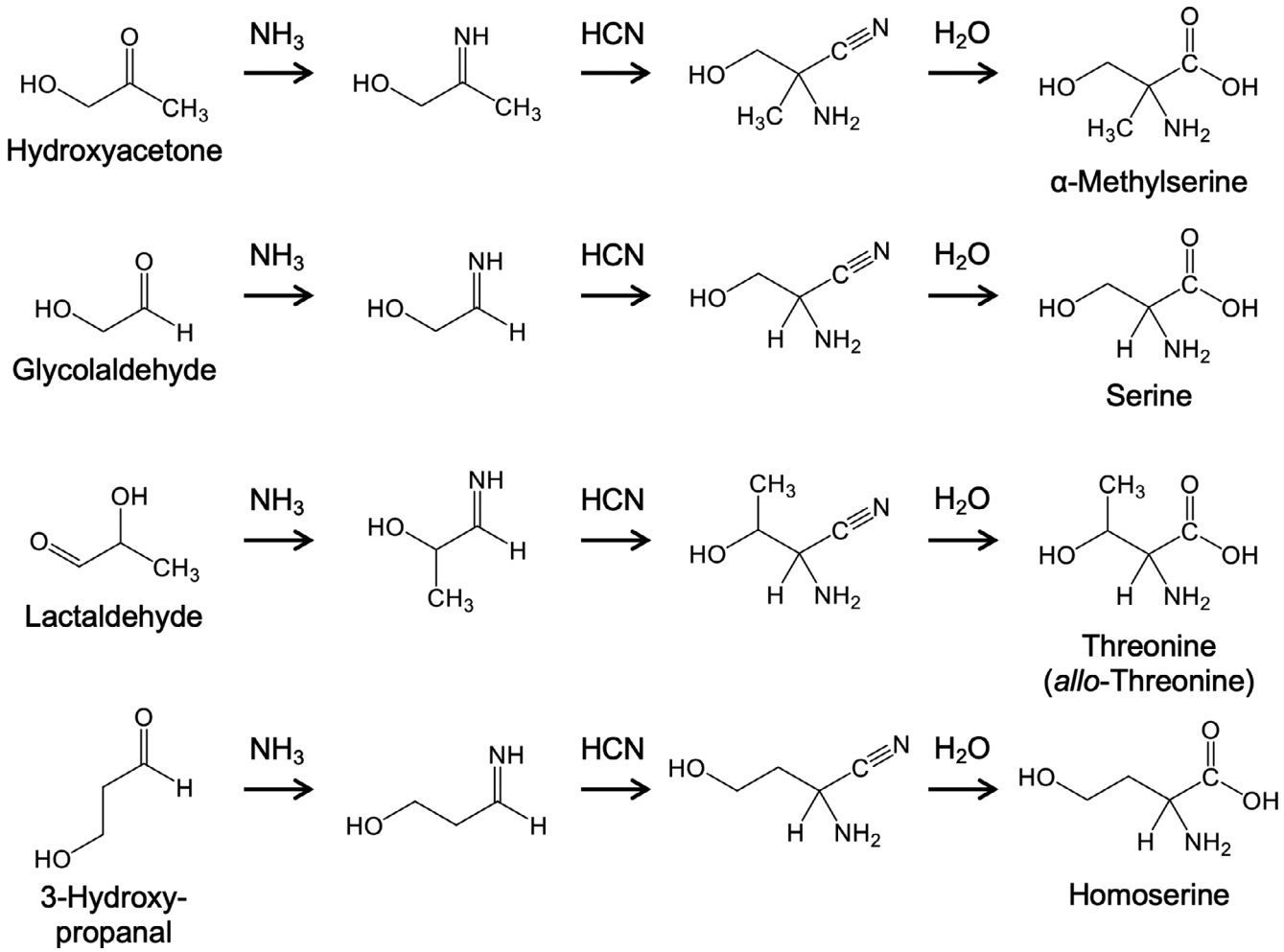

Fig. 5. Examples of the proposed synthetic pathways for the formation of select α-hydroxy amino acids via the Strecker cyanohydrin reaction. It must be noted that α-hydroxy amino acids could also be synthesized by an ammonia-involved formose-like reaction as described by Koga and Naraoka (2017).

becomes hydrolyzed to yield an α-amino acid (Peltzer and Bada 1978; Peltzer et al. 1984). However, in ammonia-depleted environments, the Strecker cyanohydrin synthesis would be more likely to proceed by forming a cyanohydrin, as opposed to an aminonitrile, where the cyanohydrin could subsequently be hydrolyzed to yield an α-hydroxy acid (Peltzer and Bada 1978; Peltzer et al. 1984). Pizzarello et al. (2010) reported that the CM2 Murchison meteorite contained a lower abundance ratio of α-amino acids to α-hydroxy acids (~1.3) than that of CR2 chondrites (8.0 for GRA 95229 and 16.0 for LAP 02342). The ammonia concentration in the Murchison meteorite was an order of magnitude smaller than those of the CR2 chondrites, 1.1–1.3 μmol g^{-1} (Pizzarello et al. 1994) and 14.1–18.9 μmol g^{-1} (Pizzarello and Holmes 2009), respectively. Thus, the observations may suggest that relatively ammonia-depleted environments (e.g., CM chondrite parent bodies similar to Murchison meteorite) favored the synthesis of α-hydroxy acids by the cyanohydrin synthesis compared to the relatively ammonia-rich environments (e.g., CR chondrite parent bodies similar to GRA 95229 and LAP 02342). Further ammonia quantifications in CM- and CR-type chondrites are needed to fully understand the synthetic reigns for the synthesis of meteoritic hydroxy acids and amino acids. In this work, the CM2 chondrites (Y-791198, A-881458, LEW 90500, and LON 94101) were found to contain smaller relative abundances of α-HAAs than the CR2 chondrites (MIL 07525, LAP 02342, and MET 00426) (Fig. 4C). One possible explanation for this observation could be the existence of differences in ammonia concentrations in the CR and CM chondrite parent bodies studied here. However, it is

Table 5. Summary of D/L ratios and L-enantiomeric excesses measured for several α-hydroxy amino acids in the HW and HCl extracts of CM and CR chondrites.[a]

	Y-791198		A-881458		LEW 90500		LON 94101		ALH 83100	
	CM2		CM2		CM2		CM2		CM1/2	
	Hot water	HCl	Hot water	HCl	Hot water	HCl	Hot water	HCl	Hot water	HCl
	D/L ratio (%Lee)	D/L ratio (%Lee)	D/L ratio (%Lee)	D/L ratio (%Lee)	D/L ratio (%Lee)	D/L ratio (%Lee)	D/L ratio (%Lee)	D/L ratio (%Lee)	D/L ratio (%Lee)	D/L ratio (%Lee)
Serine (α)	[b]	0.35 ± 0.12 (47.9 ± 10.0)	0.13 ± 0.02 (76.8 ± 1.7)	0.42 ± 0.03 (40.8 ± 2.1)	0.36 ± 0.05 (47.0 ± 4.2)	0.20 ± 0.02 (66.9 ± 2.0)	0.17 ± 0.04 (70.3 ± 4.1)	0.12 ± 0.04 (78.4 ± 4.0)	0.031 ± 0.002 (93.9 ± 0.3)	0.13 ± 0.02 (76.6 ± 1.9)
α-Methylserine (α)	1.06 ± 0.15 (−2.7 ± 7.2)	1.02 ± 0.08 (−0.9 ± 4.2)	1.03 ± 0.11 (−1.5 ± 5.3)	1.03 ± 0.04 (−1.2 ± 2.0)	1.02 ± 0.02 (−1.0 ± 0.9)	0.95 ± 0.02 (2.4 ± 0.8)	0.96 ± 0.01 (1.9 ± 0.6)	0.97 ± 0.18 (1.4 ± 9.1)	1.02 ± 0.05 (−1.0 ± 2.4)	0.95 ± 0.05 (2.4 ± 2.7)
Threonine (α)	[d]	[d]	0.15 ± 0.02 (74.2 ± 2.2)	0.02 ± 0.01 (95.2 ± 1.3)	[d]	0.18 ± 0.01 (69.2 ± 0.7)	0.11 ± 0.01 (80.7 ± 1.3)	0.032 ± 0.005 (93.8 ± 0.7)	[c]	[c]
allo-Threonine (α)	[d]	0.99 ± 0.12 (0.3 ± 6.2)	[d]	[d]	[d]	[d]	[d]	[b]	[d]	[d]
Homoserine (α)	[d]	[d]	0.96 ±.06 (2.2 ± 3.3)	[d]	[d]	1.00 ± 0.07 (0.1 ± 3.5)	[d]	0.86 ± 0.17 (7.6 ± 9.2)	0.32 ± 0.01 (51.7 ± 1.2)	0.85 ± 0.03 (8.0 ± 1.6)
	MIL 07525		LAP 02342		MET 00426		GRO 95577			
	CR2		CR2		CR2		CR1			
	Hot water	HCl	Hot water	HCl	Hot water	HCl	Hot water	HCl		
	D/L ratio (%Lee)	D/L ratio (%Lee)	D/L ratio (%Lee)	D/L ratio (%Lee)	D/L ratio (%Lee)	D/L ratio (%Lee)	D/L ratio (%Lee)	D/L ratio (%Lee)		
Serine (α)	[b]	[b]	0.92 ± 0.12 (4.2 ± 6.2)	0.99 ± 0.19 (0.5 ± 9.5)	[b]	0.84 ± 0.04 (8.6 ± 1.9)	0.13 ± 0.01 (76.6 ± 1.4)	0.22 ± 0.05 (64.2 ± 5.3)		
α-Methylserine (α)	1.11 ± 0.02 (−5.4 ± 0.8)	1.12 ± 0.18 (−5.5 ± 8.5)	1.18 ± 0.16 (−8.1 ± 7.3)	1.05 ± 0.23 (−2.6 ± 11.3)	1.10 ± 0.09 (−4.9 ± 4.3)	1.14 ± 0.02 (−6.6 ± 0.8)	0.94 ± 0.09 (3.3 ± 4.8)	1.00 ± 0.08 (0.0 ± 3.9)		
Threonine (α)	[d]	[d]	[d]	[d]	[d]	[d]	[c]	[c]		
allo-Threonine (α)	[d]	1.07 ± 0.22 (−3.2 ± 10.5)	[d]	[d]	[d]	[d]	n.d.	n.d.		
Homoserine (α)	[d]	[d]	[d]	[d]	[d]	[d]	[d]	[d]		

n.d. = not determined.

[a]The standard errors (δx) for D/L ratios and the L-enantiomeric excesses (L_{ee}) are based on the values and errors from Table 2 and Table 3 propagated through the relevant equations with Lee = ([L-D]/[L+D]) x 100.

[b]The L-enantiomeric excesses were not reported because replicate measurements of this analyte were not made.

[c]The L-enantiomeric excesses could not be calculated because the concentration of the D-enantiomer was below the detection limit.

[d]L-enantiomeric excesses were not reported due to coelution with other chromatographic peaks.

also possible that other factors may have contributed to this observed disparity. For example, different parent bodies could have evolved at dissimilar times and in disparate locations, resulting in varying synthetic yields of α-HAAs. Additionally, it is possible that α-HAAs could have been formed elsewhere in the interstellar medium prior to incorporation into meteorite parent body environments. For example, several laboratory experiments have revealed that the ultraviolet photolysis of interstellar ice analogs can yield the α-HAA serine (Bernstein et al. 2002; Muñoz Caro et al. 2002; Elsila et al. 2007; Oba et al. 2016). Nonetheless, the observation of greater α-HAA relative abundances in the CR2 extracts than the CM2 extracts analyzed here is an intriguing result that warrants further investigation to determine the genesis of this difference.

A Proposed Formation Mechanism for β-, and γ-Hydroxy Amino Acids: Ammonia-Involved Formose-Like Reaction

Previous reports suggest that the Strecker cyanohydrin synthesis can form α-amino acids, but not β- and γ-amino acids (Elsila et al. [2012] and references therein). Consequently, to explain the distribution of HAA structural isomers observed in the carbonaceous chondrites studied here, a complementary formation mechanism is required. The syntheses of α-, β-, and γ-HAAs were observed in laboratory experiments performed by Koga and Naraoka (2017), which produced a total of 17 amino acids via a formose-like reaction involving formaldehyde, acetaldehyde, glycolaldehyde, and ammonia in aqueous solution at 60 °C for 6 days. Therefore, insight into how structural diversity of HAAs may have been formed in the parent bodies of the meteorites analyzed in this study may be gleaned from a combination of the experiments outlined in Koga and Naraoka (2017) and the formose reaction. In the formose reaction, glycolaldehyde and eventually sugars are formed from the condensation of formaldehyde molecules in alkaline solution (Breslow 1959). It has been proposed that the formation of β- and γ-HAAs may follow a similar line of synthesis, whereby aldehydes (e.g., formaldehyde and glycolaldehyde), in the presence of ammonia, could yield amino acids via the formose reaction and an aldol condensation (Koga and Naraoka 2017). The nomenclature for such a formation pathway for β- and γ-HAAs could be considered an ammonia-involved formose-like reaction. Therefore, the presence of β- and γ-HAA isomers found in all the carbonaceous chondrites analyzed in this work suggests that an ammonia-involved formose-like reaction may have occurred in the parent bodies of the meteorites studied here, which could have complemented the Strecker cyanohydrin synthesis to generate HAA structural diversity. The more predominant relative abundances of β- and γ-HAAs in CM chondrites (Fig. 4C) may also suggest that a formose-like reaction could have occurred more prominently in the parent bodies of CM chondrites than CR chondrites. It is worth noting that α-amino acids could be generated not only by the Strecker cyanohydrin reaction but also by an ammonia-involved formose-like reaction since laboratory experiments conducted by Koga and Naraoka (2017) and Kebukawa et al. (2017) observed the formation of various α-amino acids from aldehydes and ammonia.

A similar reaction to an ammonia-involved formose-like reaction has been recognized to produce chondritic insoluble organic matter, such as organic solids (Kebukawa et al. 2013) and various soluble organic compounds, including N-bearing compounds (Kebukawa et al. 2020) and conventional amino acids other than HAAs (Kebukawa et al. 2017). The recent discovery of hexamethylenetetramine (HMT), and hydroxy- and hydroxymethyl- variants of HMT in CM2 meteorites (Oba et al. 2020) may suggest a relationship to facilitate an ammonia-involved formose-like reaction. Further studies to look for HMT and its variants in CR meteorites could be illuminating.

While the Strecker cyanohydrin reaction utilizes aldehydes (or ketones), ammonia, and cyanide to synthesize only α-amino acids, an ammonia-involved formose-like reaction requires only aldehydes and ammonia, but not cyanide, to produce α-, β-, and γ-HAAs. Thus, both formation mechanisms could have occurred simultaneously using the same pool of starting reagents (i.e., aldehydes and ammonia), whereas cyanide concentrations in meteorite parent bodies would influence which reaction predominated. For the Strecker cyanohydrin synthesis to have predominated, the parent body environment would have needed cyanide-rich conditions, which also include precursor aldehydes and/or ketones and ammonia to facilitate the formation of α-HAAs. Over time, HCN abundances on the parent bodies could have become depleted due to consumption via the Strecker cyanohydrin reaction, HCN polymerization (Lerner et al. 1993), and metal-cyanide complexation (Smith et al. 2019). Such HCN-poor environments may have been unfavorable for the viability of the Strecker cyanohydrin synthesis to produce α-HAAs. However, an ammonia-involved formose-like reaction occurs readily in cyanide-depleted scenarios to produce a mixture of α-, β-, and γ-HAAs from aldehydes and ammonia (Koga and Naraoka 2017). Therefore, the depletion of HCN on the meteorite parent bodies may have marked the transition from α-HAA production with relatively enhanced contributions by the Strecker cyanohydrin synthesis to

the formation of α-, β-, and γ-HAAs with relatively large contributions from an ammonia-involved formose-like reaction. In the future, laboratory experiments that simulate the conditions of the parent bodies of CM and CR chondrites, while using aldehydes, ammonia, and ^{13}C-labeled HCN, will be needed to better evaluate the relative contributions to HAA syntheses of the Strecker cyanohydrin reaction and an ammonia-involved formose-like reaction.

HAA analyses conducted in this study revealed that the relative abundances of β- and γ-HAAs in the HCl extracts were comparable to or greater than those in the HW extracts for most CM and CR chondrites (Figs. 4A and 4B). This observation may indicate that HCl extracted β- and γ-HAAs more efficiently than HW. Alternatively, it is not known whether the exposure of the meteorite sample to the HW extraction produces more α-HAAs from α-HAA precursors, or likewise for HCl exposure producing more β- and γ-HAAs from β- and γ-HAA precursors. One possible group or precursor compounds of β- and γ-HAAs are hydroxy lactams. Cooper and Cronin (1995) reported an extensive homologous series of lactams in the CM2 Murchison meteorite, suggesting that hydroxy lactams could be present in carbonaceous chondrites. In future works, the measurement of HAAs' isotopic compositions of the HW and HCl extracts is necessary to more rigorously evaluate whether solubility or synthetic considerations can explain the observed differences.

CONCLUSIONS

The research presented here entailed the analyses of five CM chondrites and four CR chondrites to examine the abundances, distributions, and enantiomeric ratios of a suite of HAAs in the HW and 6 M HCl extracts of these chondrites. To perform the necessary HAA analyses, we developed a new GC-MS analytical technique to target 13 HAAs, including α-, β-, and γ-HAAs.

The HAA analyses performed in this study revealed that distinct differences in α-HAA distributions existed between CR and CM chondrites, which are groups of chondrites with different chemistries. Elevated abundances of the α-hydroxy amino acids serine and α-methylserine were observed more prominently in the CR2 chondrites than the CM chondrites. In contrast to disproportionate α-HAA abundance comparisons between the chondrites studied here, total abundances of β- and γ-HAAs were similar between the CM and CR chondrites. The total HAA abundances of the CM and CR chondrites generally appeared to be inversely proportional to the degree of aqueous alteration in the parent bodies, as determined by the phyllosilicate fraction (Howard et al. 2015) for CM chondrites and the degree of hydration (Alexander et al. 2013) for CR chondrites, respectively. However, it is worth noting that A-881458 and MIL 07525 are not necessarily included in this assessment as these two chondrites do not currently possess a phyllosilicate fraction classification, nor a degree of hydration assessment. The chondrite ALH 83100 is also not included in this assessment due to the likely significant L-serine and L-threonine contamination observed, skewing the total HAA abundance observed for this meteorite. A plurality of non-proteinogenic HAAs, including α-methylserine, did not show enantiomeric excesses correlating with the degree of the aqueous alteration, a phenomenon previously observed in meteoritic isovaline (Glavin and Dworkin 2009). Further investigations are needed to verify observed enantiomeric excesses of α-methylserine and homoserine in select carbonaceous chondrite extracts with quantitative analyses using UPLC-FD/ToF-MS and isotopic analyses using gas chromatography combustion isotope ratio mass spectrometry.

The elevated total abundances of α-HAAs in CR2 chondrites could be produced by the Strecker cyanohydrin reaction, which may dominate under ammonia-enriched conditions in the meteorite parent body, as suggested by Pizzarello et al. (2011). The ubiquitous presence of β- and γ-HAAs in CM and CR chondrites, but more predominantly in the CM chondrites studied here, might suggest that a process similar to an ammonia-involved formose-like reaction proceeded in the meteorite parent bodies, and perhaps more so in the parent bodies of CM chondrites (Koga and Naraoka 2017) than CR chondrites. Meteoritic α-HAAs could be generated not only by the Strecker cyanohydrin reaction but also an ammonia-involved formose-like reaction. Further investigations are needed to confirm the extent to which these formation mechanisms are responsible for the HAA abundances observed in the meteorite extracts analyzed here.

Acknowledgments—This work was supported by the JSPS Overseas Challenge Program for Young Researchers Grant (number 201880018), the NASA Astrobiology Institute through award 13-13NAI7-0032 to the Goddard Center for Astrobiology, and a grant from the Simons Foundation (SCOL award 302497 to J.P.D.). We thank the National Institute of Polar Research and the Antarctic meteorite curator at the NASA Johnson Space Center for providing the meteorite samples used in this study. US Antarctic meteorite samples were recovered by the Antarctic Search for Meteorites (ANSMET) program which has

been funded by NSF and NASA and characterized and curated by the Department of Mineral Sciences of the Smithsonian Institution and the Astromaterials Curation Office at the NASA Johnson Space Center. Japanese Antarctic meteorite samples were provided by the National Institute of Polar Research (NIPR). We appreciate valuable comments on the manuscript from two anonymous reviewers. The authors declare no conflicts of interest.

Data availability statement—The data that support the findings of this study are available from the corresponding author upon reasonable request.

Editorial Handling—Dr. Scott Sandford

REFERENCES

Alexander C. M. O'D., Howard K. T., Bowden R., and Fogel M. L. 2013. The classification of CM and CR chondrites using bulk H, C and N abundances and isotopic compositions. *Geochimica et Cosmochimica Acta* 123:244–260.

Bada J. L., Glavin D. P., McDonald G. D., and Becker L. 1998. A search for endogenous amino acids in Martian meteorite ALH84001. *Science* 279:362–365.

Bernstein M. P., Dworkin J. P., Sandford S. A., Cooper G. W., and Allamandola L. J. 2002. Racemic amino acids from the ultraviolet photolysis of interstellar ice analogues. *Nature* 416:401–403.

Botta O. and Bada J. L. 2002. Extraterrestrial organic compounds in meteorites. *Surveys in Geophysics* 23:411–467.

Breslow R. 1959. On the mechanism of the formose reaction. *Tetrahedron Letters* 1:22–26.

Burton A. S., Grunsfeld S., Elsila J. E., Glavin D. P., and Dworkin J. P. 2014. The effects of parent-body hydrothermal heating on amino acid abundances in CI-like chondrites. *Polar Science* 8:255–263.

Chyba C. and Sagan C. 1992. Endogenous production, exogenous delivery and impact-shock synthesis of organic molecules: An inventory for the origins of life. *Nature* 355:125–132.

Cooper G. W. and Cronin J. R. 1995. Linear and cyclic aliphatic carboxamides of the Murchison meteorite: Hydrolyzable derivatives of amino acids and other carboxylic acids. *Geochimica et Cosmochimica Acta* 59:1003–1015.

Elsila J. E., Dworkin J. P., Bernstein M. P., Martin M. P., and Sandford S. A. 2007. Mechanisms of amino acid formation in interstellar ice analogs. *The Astrophysical Journal* 660:911–918.

Elsila J. E., Charnley S. B., Burton A. S., Glavin D. P., and Dworkin J. P. 2012. Compound-specific carbon, nitrogen, and hydrogen isotopic ratios for amino acids in CM and CR chondrites and their use in evaluating potential formation pathways. *Meteoritics & Planetary Science* 47:1517–1536.

Elsila J. E., Aponte J. C., Blackmond D. G., Burton A. S., Dworkin J. P., and Glavin D. P. 2016. Meteoritic amino acids: Diversity in compositions reflects parent body histories. *ACS Central Science* 2:370–379.

Engel M. H. and Nagy B. 1982. Distribution and enantiomeric composition of amino acids in the Murchison meteorite. *Nature* 296:837–840.

Glavin D. P. and Dworkin J. P. 2009. Enrichment of the amino acid L-isovaline by aqueous alteration on Cl and CM meteorite parent bodies. *Proceedings of the National Academy of Sciences of the United States of America* 106:5487–5492.

Glavin D. P., Bada J. L., Brinton K. L. F., and McDonald G. D. 1999. Amino acids in the Martian meteorite Nakhla. *Proceedings of the National Academy of Sciences* 96:8835–8838.

Glavin D. P., Dworkin J. P., Aubrey A., Botta O., Doty J. H., Martins Z., and Bada J. L. 2006. Amino acid analyses of Antarctic CM2 meteorites using liquid chromatography-time of flight-mass spectrometry. *Meteoritics & Planetary Science* 41:889–902.

Glavin D. P., Callahan M. P., Dworkin J. P., and Elsila J. E. 2010. The effects of parent body processes on amino acids in carbonaceous chondrites. *Meteoritics & Planetary Science* 45:1948–1972.

Glavin D. P., Alexander C. M. O'D., Aponte J. C., Dworkin J. P., Elsila J. E., and Yabuta H. 2018. The origin and evolution of organic matter in carbonaceous chondrites and links to their parent bodies. In *Primitive meteorites and asteroids,* edited by Abreu N. Amsterdam, the Netherlands: Elsevier, pp. 205–271.

Glavin D. P., Elsila J. E., McLain H. L., Aponte J. C., Parker E. T., Dworkin J. P., Hill D. H., Connolly H. C., and Lauretta D. S. 2020a. Extraterrestrial amino acids and L-enantiomeric excesses in the CM2 carbonaceous chondrites Aguas Zarcas and Murchison. *Meteoritics & Planetary Science* 26:1–26.

Glavin D. P., McLain H. L., Dworkin J. P., Parker E. T., Elsila J. E., Aponte J. C., Simkus D. N., Pozarycki C. I., Graham H. V., Nittler L. R., and Alexander C. M. O'D. 2020b. Abundant extraterrestrial amino acids in the primitive CM carbonaceous chondrite Asuka 12236. *Meteoritics & Planetary Science* 55:1979–2006.

Harju E. R., Rubin A. E., Ahn I., Choi B.-G., Ziegler K., and Wasson J. T. 2014. Progressive aqueous alteration of CR carbonaceous chondrites. *Geochimica et Cosmochimica Acta* 139:267–292.

Howard K. T., Alexander C. M. O'D., Schrader D. L., and Dyl K. A. 2015. Classification of hydrous meteorites (CR, CM and C2 ungrouped) by phyllosilicate fraction: PSD-XRD modal mineralogy and planetesimal environments. *Geochimica et Cosmochimica Acta* 149:206–222.

Kebukawa Y., Kilcoyne A. L. D., and Cody G. D. 2013. Exploring the potential formation of organic solids in chondrites and comets through polymerization of interstellar formaldehyde. *The Astrophysical Journal* 771:19.

Kebukawa Y., Chan Q. H. S., Tachibana S., Kobayashi K., and Zolensky M. E. 2017. One-pot synthesis of amino acid precursors with insoluble organic matter in planetesimals with aqueous activity. *Science Advances* 3:e1602093.

Kebukawa Y., Nakashima S., Mita H., Muramatsu Y., and Kobayashi K. 2020. Molecular evolution during hydrothermal reactions from formaldehyde and ammonia simulating aqueous alteration in meteorite parent bodies. *Icarus* 347:113827.

Kimura M., Grossman J. N., and Weiserg M. K. 2011. Fe-Ni metal and sulfide minerals in CM chondrites: An indicator for thermal history. *Meteoritics & Planetary Science* 46:431–442.

Koga T. and Naraoka H. 2017. A new family of extraterrestrial amino acids in the Murchison meteorite. *Scientific Reports* 7:1–8.

Lerner N. R. and Cooper G. W. 2005. Iminodicarboxylic acids in the Murchison meteorite: Evidence of Strecker reactions. *Geochimica et Cosmochimica Acta* 69:2901–2906.

Lerner N. R., Peterson E., and Chang S. 1993. The Strecker synthesis as a source of amino acids in carbonaceous chondrites: Deuterium retention during synthesis. *Geochimica et Cosmochimica Acta* 57:4713–4723.

Li J., and Brill T. B. 2003. Spectroscopy of hydrothermal reactions, part 26: kinetics of decarboxylation of aliphatic amino acids and comparison with the rates of racemization. *International Journal of Chemical Kinetics* 35:602–610.

Martins Z., Modica P., Zanda B., and D'Hendecourt L. L. S. 2015. The amino acid and hydrocarbon contents of the Paris meteorite: Insights into the most primitive CM chondrite. *Meteoritics & Planetary Science* 50:926–943.

Matsuo Y. and Greenberg D. M. 1955. Metabolic formation of homoserine and alpha-aminobutyric acid from methionine. *The Journal of Biological Chemistry* 215:547–554.

Muñoz Caro G. M., Meierhenrich U. J., Schutte W. A., Barbier B., Arcones Segovia A., Rosenbauer H., Thiemann W.-H.-P., Brack A., and Greenberg J. M. 2002. Amino acids from ultraviolet irradiation of interstellar ice analogues. *Nature* 416:403–406.

Nakamura T. 2005. Post-hydration thermal metamorphism of carbonaceous chondrites. *Journal of Mineralogical and Petrological Sciences* 100:260–272.

Oba Y., Takano Y., Naraoka H., Furukawa Y., Glavin D. P., Dworkin J. P., and Tachibana S. 2020. Extraterrestrial hexamethylenetetramine in meteorites—A precursor of prebiotic chemistry in the inner solar system. *Nature Communications* 11:6243.

Oba Y., Takano Y., Watanabe N., and Kouchi A. 2016. Deuterium fractionation during amino acid formation by photolysis of interstellar ice analogs containing deuterated methanol. *The Astrophysical Journal* 827:L18.

Peltzer E. T. and Bada J. L. 1978. α-Hydroxycarboxylic acids in the Murchison meteorite. *Nature* 272:443–444.

Peltzer E. T., Bada J. L., Schlesinger G., and Miller S. L. 1984. The chemical conditions on the parent body of the murchison meteorite: Some conclusions based on amino, hydroxy and dicarboxylic acids. *Advances in Space Research* 4:69–74.

Pizzarello S. and Holmes W. 2009. Nitrogen-containing compounds in two CR2 meteorites: 15N composition, molecular distribution and precursor molecules. *Geochimica et Cosmochimica Acta* 73:2150–2162.

Pizzarello S., Feng X., Epstein S., and Cronin J. R. 1994. Isotopic analyses of nitrogenous compounds from the Murchison meteorite: Ammonia, amines, amino acids, and polar hydrocarbons. *Geochimica et Cosmochimica Acta* 58:5579–5587.

Pizzarello S., Zolensky M., and Turk K. A. 2003. Nonracemic isovaline in the Murchison meteorite: Chiral distribution and mineral association. *Geochimica et Cosmochimica Acta* 67:1589–1595.

Pizzarello S., Wang Y., and Chaban G. M. 2010. A comparative study of the hydroxy acids from the Murchison, GRA 95229 and LAP 02342 meteorites. *Geochimica et Cosmochimica Acta* 74:6206–6217.

Pizzarello S., Williams L. B., Lehman J., Holland G. P., and Yarger J. L. 2011. Abundant ammonia in primitive asteroids and the case for a possible exobiology. *Proceedings of the National Academy of Sciences* 108:4303–4306.

Pizzarello S., Schrader D. L., Monroe A. A., and Lauretta D. S. 2012. Large enantiomeric excesses in primitive meteorites and the diverse effects of water in cosmochemical evolution. *Proceedings of the National Academy of Sciences of the United States of America* 109:11,949–11,954.

Pollock G. E., Cheng C.-N., Cronin S. E., and Kvenvolden K. A. 1975. Stereoisomers of isovaline in the Murchison meteorite. *Geochimica et Cosmochimica Acta* 39:1571–1573.

Rubin A. E., Trigo-Rodríguez J. M., Huber H., and Wasson J. T. 2007. Progressive aqueous alteration of CM carbonaceous chondrites. *Geochimica et Cosmochimica Acta* 71:2361–2382.

Simkus D. N., Aponte J. C., Elsila J. E., Parker E. T., Glavin D. P., and Dworkin J. P. 2019. Methodologies for analyzing soluble organic compounds in extraterrestrial samples: Amino acids, amines, monocarboxylic acids, aldehydes, and ketones. *Life* 9:47.

Smith K. E., House C. H., Arevalo R. D., Dworkin J. P., and Callahan M. P. 2019. Organometallic compounds as carriers of extraterrestrial cyanide in primitive meteorites. *Nature Communications* 10:1–7.

Vollmer C., Pelka M., Leitner J., and Janssen A. 2020. Amorphous silicates as a record of solar nebular and parent body processes—A transmission electron microscope study of fine-grained rims and matrix in three Antarctic CR chondrites. *Meteoritics & Planetary Science* 55:1979–2006.

SUPPORTING INFORMATION

Additional supporting information may be found in the online version of this article.

Table S1. Summary of the fragment ions (m/z) used for quantification of each HAA in the CM and CR chondrites.

Table S1. Summary of the fragment ions (*m/z*) used for quantification of each HAA in the CM and CR chondrites.

	Y-791198 CM2		A-881458 CM2		LEW 90500 CM2		LON 94101 CM2		ALH 83100 CM1/2		MIL 07525 CR2		LAP 02342 CR2		MET 00426 CR2		GRO 95577 CR1	
Hydroxy amino acids (Peak # in Fig. 2, 3)	HW	HCl	HW	HCl	HW	HCl	HW	HCl	HW	HCl	HW	HCl	HW	HCl	HW	HCl	HW	HCl
D-Serine (#1)	239	239	239	239	239	239	239	239	239	239	239	239	239	239	239	239	239	239
L-Serine (#2)	239	239	284	239	239	239	239	239	239	239	239	239	239	239	239	239	239	239
DL-Isoserine (#3 & 4)	452	239	239	239	239	452	239	452	452	239	239	239	452	452	239	452	239	239
L-α-Methylserine (#5)	252	252	252	252	252	252	252	252	252	252	252	252	252	252	252	252	252	252
D-α-Methylserine (#6)	252	252	252	252	252	252	252	252	252	252	252	252	252	252	252	252	252	252
D-Threonine (#7)	253	253	253	253	253	253	253	253	n.d.	n.d.	253	253	253	253	253	253	n.d.	n.d.
L-Threonine (#8)	253	253	253	253	253	253	253	253	253	253	253	253	253	253	253	253	253	253
Isothreonine (#9)	466	466	466	466	466	466	466	466	n.d.	n.d.	466	466	466	466	466	466	n.d.	n.d.
Isothreonine (#10)	466	466	466	466	466	466	466	466	n.d.	n.d.	466	466	466	466	466	466	n.d.	n.d.
DL-α-Methylisoserine (#11)	466	252	466	252	252	466	252	466	252	252	466	466	466	466	466	466	252	252
D-*allo*-Threonine (#12)	253	253	253	253	253	253	253	253	253	253	466	298	238	253	466	252	n.d.	n.d.
L-*allo*-Threonine (#13)	253	253	253	253	253	253	253	253	253	253	466	298	238	253	466	252	n.d.	n.d.
allo-Isothreonine (#14)	272	466	272	272	272	272	272	272	272	n.d.	272	272	272	272	272	272	n.d.	n.d.
allo-Isothreonine (#15)	272	466	272	272	272	272	272	272	272	n.d.	272	272	272	272	272	272	n.d.	n.d.
D-Homoserine (#16)	252	252	298	252	252	252	252	252	252	252	252	252	252	252	252	252	252	252
L-Homoserine (#17)	252	252	298	252	252	252	252	252	252	252	252	252	252	252	252	252	252	252
DL-β-Homoserine (#18)	494	494	494	n.d.	494	494	494	494	494	n.d.	494	494	494	494	494	494	n.d.	n.d.
D-3-A-2-HMPA (#19)	280	280	280	280	n.d.	280	n.d.	280	n.d.	n.d.	n.d.	280	n.d.	280	n.d.	280	n.d.	n.d.
L-4-A-2-HBA (#20)	466	466	466	466	n.d.	466	n.d.	466	n.d.	466	n.d.	466	n.d.	466	n.d.	466	466	466
D-4-A-3-HBA (#21)	252	252	280	252	n.d.	252	n.d.	252	n.d.	252	n.d.	280	n.d.	252	n.d.	280	252	n.d.
L-4-A-3-HBA (#22)	252	252	280	252	n.d.	252	n.d.	252	n.d.	252	n.d.	280	n.d.	252	n.d.	280	252	n.d.

n.d. = value not determined due to trace amino acid abundances.